Exact Symbol Error Rate of Frequency-Hopped MPSK under Rician Fading and Partial Band Tone Jamming

, Matthew R. Hannon, Akarsh S. Pokkunuru, Edwin Tambi, Shuang Feng, Hyuck Kwon
Department of Electrical Engineering and Computer Science,
Wichita State University, Wichita, Kansas 67260-0083

Khanh Pham and Steven Lane
Air Force Research Laboratory
Kirtland Air Force Base, NM 87117-57768

Abstract — This paper considers a coherent (instead of non-coherent) modulation such as an M-ary phase-shift keying (MPSK) and M-ary quadrature amplitude-shift keying (MQAM) for a slow frequency hopping spread spectrum (FHSS) system. Then, this paper presents an exact symbol error rate (SER) expression for the FHSS system under partial-band tone jamming (PBTJ) and Rician fading environments through analysis. In addition, this paper studies the optimal weighting coefficients for each hop interval to minimize the SER. Furthermore, this paper derives an implicit expression of the optimal PBTJ fraction ratio, which maximizes the SER of the FHSS system and compares the analytical results with the numerical results for verification. The results shown here can be useful for an efficient FHSS satellite and mobile communications system design when a coherent FHSS modulation is employed under severe fading as well as severe PBTJ environments.

Index Terms—Frequency hopping, spread spectrum, coherent modulation, Rician fading, partial band tone jamming, and symbol error rate.

I. Introduction

In today's fast-paced world, connectivity is of prime importance to everyone. Not only being connected to everyone but faster access of data through the cloud or any other medium is a necessity. Various techniques have been proven to deploy a fast and efficient network. Technologies such as wideband-code division multiple access (W-CDMA), high-speed downlink

packet access (HSDPA), long-term evolution (LTE), and LTE-Advanced have been popular for high-speed mobile communications [1]-[3]. But, the question to ask is whether or not the connection to the network or other users would be secure or not.

Due to the presence of various malicious activities, such as jamming and eavesdropping, it is vital to have an error-free and secure transmission. Eavesdropping is a very serious issue since the user's privacy can be in jeopardy and result in an enormous loss of information. One of the most effective jamming attacks is partial-band tone jamming (PBTJ) or partial-band noise jamming (PBNJ) [4], [5]. Both are equivalent, and the PBTJ is more effective but can be exposed to friendly users more than PBNJ. This paper considers PBTJ, which reduces system symbol error rate (SER) performance and degrades throughput efficiency by reducing the effective signal-to-noise ratio (SNR) of the user. A successful solution to this issue can be addressed by moving into the 2.4 GHz frequency band, where spread spectrum communication operates [6]-[8]. Spread spectrum communication is a vital technique for establishing secure connections among various applications including the military as well as commercial mobile communications.

Some of the most commonly used military radios that make use of frequency hopping belong to the joint tactical information distribution system (JTIDS), multifunctional information distribution system (MIDS), and single-channel ground and airborne radio system (SINCGARS) [9]-[11]. The preference of operation is given to frequency hopping spread spectrum (FHSS) communication because it is difficult to intercept messages due to the presence of a pseudo random sequence key generation in transmission security (TRANSEC) in every message [12].

Other advantages of FHSS communication are that it is very bandwidth efficient, error control is possible, and the cost is low because components are readily available. Thus, because of these advantages, this paper uses slow FHSS communication in the presence of a PBTJ jamming scenario. Here, a slow frequency hopping (FH) means multiple symbols transmitted per hop. Again, the existing FH pattern design employs both a hopping keystream and a time permutation keystream for resistance to jamming and detection. The entire hopping spectrum is uniformly occupied over a large number of hops. Hence, we assume a random FH pattern, which is good, in order to cause a low probability of detection. However, the probability of a hit by a single-tone jammer for the random FH pattern is high such as $1/N_f$, where N_f denotes the total number of frequency positions in the entire hopping spectrum. Once a desired narrow band signal is hit by a tone jammer with sufficient jamming power, half of the symbols in the hop are likely to be in

error for a binary modulation. If a jammer has sufficient power, then it can generate multiple tones instead of a single tone. This is why we consider PBTJ and want to determine the optimum PBTJ fraction ratio for a given jamming power constraint.

Between late 1970 and early 1990, FHSS communications systems under various types of jamming have been studied [13]-[17], considering non-coherent modulations such as M-ary frequency-shift keying (MFSK) and M-ary differential phase-shift keying (MDPSK). For example, in [15], the authors presented a method for calculating MDPSK error probability in PBTJ and additive white Gaussian noise (AWGN). Also, Rician fading was considered. In [16], the authors studied FHSS with binary non-coherent frequency-shift keying (FSK) in a shadowed Rician fading and the PBTJ. The Chernoff upper bound was used for the bit error probability derivation. The reason why the coherent modulation such as M-ary phase-shift keying (MPSK) was not employed for the FH system in those days was because of implementation issues, such as a frequency-ringing problem, which occurred whenever a frequency was hopped to a new frequency.

Today, these implementation technologies have improved, and MPSK has been considered for future protected tactical waveform (PTW) FH systems to achieve further bandwidth efficiency over the non-coherent MFSK modulation [18], [19]. However, there has not been an exact symbol error rate (SER) analysis of FH/MPSK under PBTJ and Rician fading. This paper presents an exact SER of the FH/MPSK under PBTJ and Rician fading using the moment generation function (MGF) [20], [21]. Numerical SER results of the FH/MPSK under Rician fading and PBTJ are presented. The analysis in this paper can be extended for other coherent modulations such as M-ary quadrature amplitude modulation (MQAM), other mobile fading environments such as Nakami and Rayleigh, and other jamming such as PBNJ without difficulty. Corresponding SER expressions for other coherent modulations and other channel environments are simply presented without numerical results in this paper. Optimal weighting coefficients for each hop interval are also considered. Furthermore, the optimal PBTJ fraction ratio is derived and compared with numerical results. Results in this paper can be useful for efficient FHSS satellite and mobile communications system designs when a coherent FHSS modulation is employed under severe fading as well as a severe PBTJ environment.

The rest of the paper is organized as follows: Sections II describes the system model. Then, Section III presents an exact SER expression of the FH/MPSK under the AWGN, PBTJ, and

Rician fading. Section IV finds an expression to determine the optimum PBTJ fraction. Section V shows numerical results, and Section VI concludes the paper.

Notations: The upper-bar, e.g., $\overline{X}$, denotes the average value of a random variable X; $E[X]$ also denotes the expectation or average of a random variable X; the bold lower case, e.g., $\boldsymbol{x}$ denotes a vector; $\boldsymbol{x}^T$ denotes the transpose of vector $\boldsymbol{x}$; $\|\boldsymbol{x}\|$ denotes the norm of vector $\boldsymbol{x}$; and $|x|$ denotes the magnitude of a complex number x.

II. System model

The entire FH spectrum is divided into N_f number of channels operating at frequencies $f_1, \cdots,$ and f_{N_f}. All channels are independent of each other and have a hop interval denoted by T_h. One data frame consists of L_h number of time hops. Since a slow frequency hopping is considered, N_s multiple symbols are transmitted per hop. For example, Fig. 1 shows an FH/MPSK of $N_f = 3$ frequency channels, $L_h = 2$ time hops per frame, $N_s = 2$ number of symbols per hop, and $N_u = 2$ number of multiple access (MA) users sharing the entire FH spectrum.

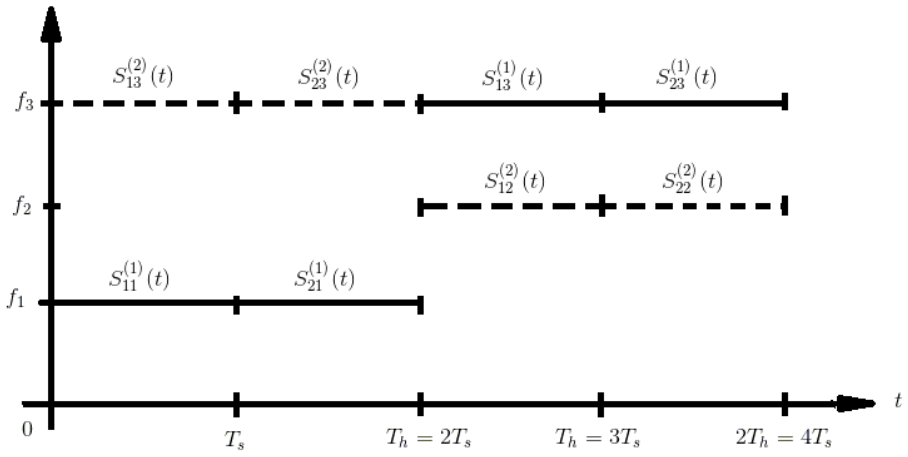

Fig. 1. Hopping patterns for $N_u = 2$ users, $N_s = 2$ symbols/hop, $N_f = 3$ frequencies, and $L_h = 2$ time hops per frame.

The transmitted signal for the *k*-th user is denoted by $s_{ij}^{(k)}(t)$, where the superscript *k* denotes the user index, and subscripts *i* and *j* indicate the symbol index and frequency index in a hop, respectively. In Fig. 1, user 1's signals are $s_{11}^{(1)}(t)$ and $s_{21}^{(1)}(t)$ for the hop 1 interval, and $s_{13}^{(1)}(t)$ and $s_{23}^{(1)}(t)$ for the hop 2 interval, and user 2's signals are $s_{13}^{(2)}(t)$ and $s_{23}^{(2)}(t)$ for the hop 1

interval, and $s_{12}^{(2)}(t)$ and $s_{22}^{(2)}(t)$ for the hop 2 interval. Without loss of generality in analysis, consider that user 1 uses frequency f_1 during hop 1. The transmitted MPSK signal by user 1 can be written as

$$s_{11}^{(1)}(t) = Ag(t)cos\left[\frac{2\pi(i-1)}{M}\right]cos[2\pi f_1 t] - Ag(t)sin\left[\frac{2\pi(i-1)}{M}\right]sin[2\pi f_1 t], i = 1, \cdots, M \quad (1)$$

where $0 \le t \le T_s$, A is the amplitude of the signal, $g(t)$ is the waveform shaping filter, and i denotes the transmitted symbol out of M possible symbols.

Rician fading is assumed with channel coefficient $h_1 = |h_1|e^{j\theta_1}$, where $|h_1|$ and θ_1 are the Rician amplitude and the uniformly distributed angle of h_1, respectively [22]. It is also assumed that the transmitter is constantly under attack by PBTJ. The PBTJ signal $j(t)$ during the first hop interval $0 \le t \le T_h$ against user 1's signal is written as

$$j(t) = \begin{cases} A_J cos\left[2\pi f_1 t + \emptyset_J\right] - A_J sin\left[2\pi f_1 t + \emptyset_J\right] & \text{if user 1's signal is jammed} \\ 0 & \text{else} \end{cases} \quad (2)$$

where A_J is the amplitude of the jamming tone signal, and $\emptyset_J$ is the jamming signal phase with uniform distribution $\emptyset_J \sim (0, 2\pi)$.

Fig. 2 shows the receiver block diagram for user 1, hop 1, FH frequency f_1, and symbol 1. The received output signal from the band-pass filter (BPF) is multiplied by a receiver post processing gain α_1 if a single antenna is employed or a receiver spatial domain beam-forming (SDBF) vector $\boldsymbol{\alpha} = (\alpha_1, \cdots, \alpha_M)^T$ if M number of multiple antennas are used. We assume a single antenna receiver and Rician fading with channel efficient h_1, which can be estimated through the inserted pilot or reference symbols in a frame. Then, we can set $\alpha_1 = a_1 e^{-j\theta_1}$ because of the available channel state information and can choose a_1 to maximize the received signal-to-jamming plus noise power ratio (SJNR) γ. The BPF and post-processing signal can be written as

$$r(t) = \left[h_1 s_{11}^{(1)}(t) + j_1(t) + n_1(t)\right]\alpha_1 = |h_1|a_1 s_{11}^{(1)}(t) + j_1(t)a_1 e^{-j\theta_1} + n_1(t)a_1 e^{-j\theta_1}. \quad (3)$$

Then, the received signal $r(t)$ is down-converted in frequency to in-phase (I) and quadrature-phase (Q) baseband signal components using two orthonormal basis functions, $\emptyset_1(t)$ and $\emptyset_2(t)$, and passed through the filters matched to the waveform-shaping filter $g(t)$. Then, samples are taken of every symbol interval at each I and Q branch. Let r_1 and r_2 denote I and Q branch samples, respectively. Let $\boldsymbol{r} = (r_1, r_2)^T$, $\boldsymbol{s} = (s_1, s_2)^T$, $\boldsymbol{j} = (j_1, j_2)^T$, and $\boldsymbol{n} = (n_1, n_1)^T$ denote the received signal, the transmitted signal component, the jamming signal component, and the

noise component vector, respectively. Here, $r_i = \langle r(t), \emptyset_i(t) \rangle$ is an inner product of $r(t)$ and $\emptyset_i(t)$, which is the projection of the received signal into the base function $\emptyset_i(t)$, $i = 1,2$.

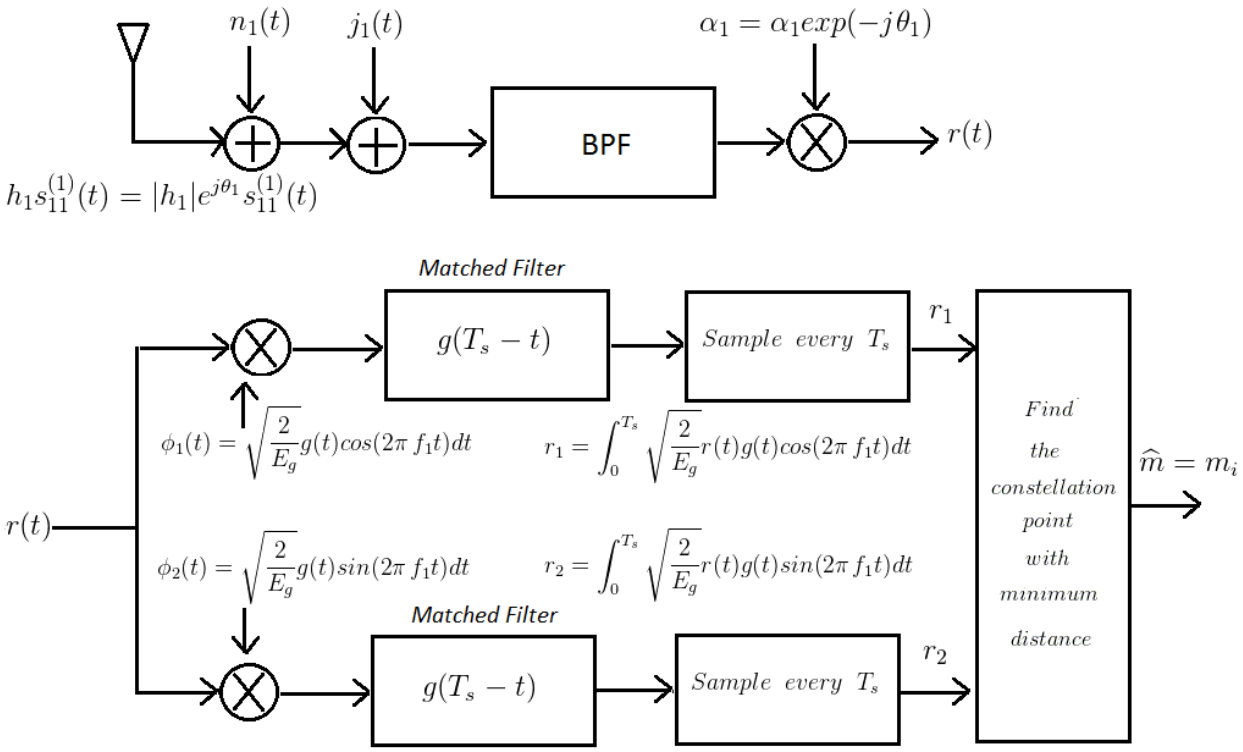

Fig. 2. Receiver for user 1, hop 1, FH frequencyf_1, and symbol 1.

The received signal vector can be written as

$$\boldsymbol{r} = \begin{cases} |h_1| a_1 \boldsymbol{s} + a_1 \boldsymbol{j} + a_1 \boldsymbol{n} & if\ jammed \\ |h_1| a_1 \boldsymbol{s} + a_1 \boldsymbol{n} & if\ unjammed \end{cases}. \tag{4}$$

Hence, the received SJNR or signal-to-noise power ratio (SNR) γ, depending on the jamming conditions, can be written as

$$\gamma = \begin{cases} \frac{E[\||h_1| a_1 \boldsymbol{s}\|^2]}{E[\|a_1 \boldsymbol{j} + a_1 \boldsymbol{n}\|^2]} = \frac{(|h_1| a_1)^2 P_S}{(a_1)^2 (P_J + P_N)} & if\ jammed \\ \frac{E[\||h_1| a_1 \boldsymbol{s}\|^2]}{E[\|a_1 \boldsymbol{n}\|^2]} = \frac{(|h_1| a_1)^2 P_S}{(a_1)^2 P_N} & if\ unjammed \end{cases} \tag{5}$$

where $P_S = E[\|\boldsymbol{s}\|^2]$, $P_J = E[\|\boldsymbol{j}\|^2]$, and $P_N = E[\|\boldsymbol{n}\|^2]$ denote the signal component, the jamming component, and noise component power, respectively. By applying the Cauchy-Schwartz inequality to (5), (i.e., $|\langle \boldsymbol{x}, \boldsymbol{y} \rangle|^2 \leq \|\boldsymbol{x}\|^2 \|\boldsymbol{y}\|^2$ with "=" if and only if $\boldsymbol{x} = c\boldsymbol{y}$ for any

constant c), the maximum γ can be achieved when a_1 is proportional to $|h_1|$. Hence, we choose a_1 as

$$a_1 = \begin{cases} \frac{|h_1|}{\sqrt{P_J+P_N}} & if\ jammed \\ \frac{|h_1|}{\sqrt{P_N}} & if\ unjammed \end{cases}. \quad (6)$$

Note that $(a_1)^2$ in (5) can directly cancel each other in the numerator and the denominator. However, when the receiver employs M_r number of multiple antennas, the terms $(|h_1|a_1)^2$ and $(a_1)^2$ used for the single-antenna case in the numerator and denominator of (5) will be changed to $\left(\sum_{i=1}^{M_r}|h_i|a_i\right)^2$ and $\sum_{i=1}^{M_r} a_i^2$, respectively. Therefore, the Cauchy-Schwartz inequality will be useful to determine the optimum weighting vector $\boldsymbol{a} = (a_1, \cdots, a_{M_r})^T$, which is proportional to the channel magnitude vector $\boldsymbol{h}_{mag} = \left(|h_1|, \cdots, |h_{M_r}|\right)^T$. Then, when the optimum weighting vector is used, the maximum SJNR or maximum SNR can be written as

$$\gamma_{max} = \begin{cases} \frac{(|h_1|)^2 P_S}{(P_J+P_N)} & if\ jammed \\ \frac{(|h_1|)^2 P_S}{P_N} & if\ unjammed \end{cases}. \quad (5)$$

Here, the noise component power can be written as

$$P_N = N_0 B = N_0 \frac{1}{T_s}. \quad (6)$$

This is because the signal channel bandwidth B is approximately equal to $1/T_s$. Let W denote the entire FH spectrum bandwidth. Then, $W = N_f B$. And the PBTJ power per tone can be written as

$$P_J = A_J^2 = \frac{P_{J,total}}{Number\ of\ PBTJ\ tones\ in\ W} = \frac{P_{J,total}}{\beta\frac{W}{B}} = \frac{N_J B}{\beta} = \frac{N_J}{\beta T_s} \quad (7)$$

where β denotes the jamming fraction ratio, $0 < \beta \leq 1$, and N_J denotes the jamming power spectral density, which is

$$N_J = \frac{P_{J,total}}{W}. \quad (8)$$

Assume a random FH pattern in this paper. Then, the jamming fraction ratio β is equal to the probability of a frequency tone being jammed. This is because

$$Pr(A\ signal\ tone\ is\ jammed\ by\ PBTJ\ ) = \frac{Number\ of\ Tones\ Jammed\ by\ PBTJ}{Total\ Number\ of\ Tones} = \frac{\beta\frac{W}{B}}{\frac{W}{B}} = \beta. \quad (9)$$

Hence, γ_{max} in (5) can be rewritten as

$$\gamma_{max} = \begin{cases} \frac{(|h_1|)^2 P_S}{\left(\frac{N_J}{\beta T_s} + N_0 \frac{1}{T_s}\right)} = \frac{(|h_1|)^2 E_S}{\left(\frac{N_J}{\beta} + N_0\right)} = \frac{(|h_1|)^2}{\left(\frac{1}{\beta E_S/N_J} + \frac{1}{E_S/N_0}\right)} & if\ jammed\ w/\ probability\ \beta \\ \frac{(|h_1|)^2 P_S}{N_0 \frac{1}{T_s}} = \frac{(|h_1|)^2 E_S}{N_0} & if\ unjammed\ w/\ probability\ (1-\beta) \end{cases} . \quad (10)$$

The purpose of PBTJ is to minimize γ, whereas the purpose of receiver beam forming (BF) is to maximize γ. We can consider the min-max problem as

$$min_{\beta, 0<\beta\leq 1}\ max_{a_1 \geq 0} = \gamma(a_1, \beta). \quad (11)$$

III. Exact Symbol Error Rate Analysis

For a given instantaneous SNR or SJNR γ, the exact SER of FH MPSK under PBTJ and Rician fading can be obtained using Craig's formula in [23] as

$$P_s(E|\gamma) = \frac{1}{\pi} \int_0^{(M-1)\pi/M} exp\left[\frac{-g\gamma}{sin^2 \emptyset}\right] d\emptyset \quad (12)$$

where

$$g = sin^2 \frac{\pi}{M}. \quad (13)$$

The average SER of FH MPSK over Rician fading and the jamming state random variable J can be written as

$$\bar{P}_s(E) = E_{\gamma,J}[P_s(E|\gamma, J)] = E_{\gamma_J}\left[P_s\left(E\middle|\gamma_J, J=1\right)\right] Pr[J=1] + E_{\gamma_N}[P_s(E|\gamma_N, J=0)] Pr[J=0] \quad (14)$$

where $J = 1$ and $J = 0$ denote the presence and absence of PBTJ, respectively, at the desired signal tone and hop of interest; hence, $Pr[J=1]$ and $Pr[J=0]$ would be β and $(1-\beta)$, respectively. And the SJNR and SNR are written, respectively, as

$$\gamma_J = \frac{(|h_1|)^2}{\left(\frac{1}{\beta E_S/N_J} + \frac{1}{E_S/N_0}\right)} \quad (14)$$

and

$$\gamma_N = \frac{(|h_1|)^2 E_S}{N_0}. \quad (15)$$

Note that both γ_J and γ_N are Rician fading. And

$$E_{\gamma_J}\left[P_s\left(E\middle|\gamma_J, J=1\right)\right] = \int_0^\infty P_s\left(E\middle|\gamma_J, J=1\right) p_{\gamma_J}(\gamma_J) d\gamma_J$$

$$= \int_0^\infty \frac{1}{\pi} \int_0^{(M-1)\pi/M} exp\left[\frac{-g\gamma_J}{sin^2 \emptyset}\right] d\emptyset\, p_{\gamma_J}(\gamma_J) d\gamma_J = \frac{1}{\pi} \int_0^{(M-1)\pi/M} \int_0^\infty exp\left[\frac{-g\gamma_J}{sin^2 \emptyset}\right] p_{\gamma_J}(\gamma_J) d\gamma_J d\emptyset$$

$$= \frac{1}{\pi} \int_0^{(M-1)\pi/M} \int_0^\infty exp\left[\frac{-g\gamma_J}{sin^2 \emptyset}\right] p_{\gamma_J}(\gamma_J) d\gamma_J d\emptyset = \frac{1}{\pi} \int_0^{(M-1)\pi/M} M_{\gamma_J}\left(\frac{-g}{sin^2 \emptyset}\right) d\emptyset$$

$$= \frac{1}{\pi}\int_0^{(M-1)\pi/M} \frac{(1+K)}{(1+K)+\frac{g}{sin^2\emptyset}\bar{\gamma}_J} \exp\left[\frac{-K\frac{g}{sin^2\emptyset}\bar{\gamma}_J}{(1+K)+\frac{g}{sin^2\emptyset}\bar{\gamma}_J}\right] d\emptyset \tag{16}$$

where $M_{\gamma_J}(s)$ is the MGF of γ_J, i.e., $M_{\gamma_J}(s) = E_{\gamma_J}[e^{s\gamma_J}]$. From [23], the MGFs for various fading environments can be written as follows:

a) For Rayleigh fading,

$$M_{\gamma_J}\left(\frac{-g}{sin^2\emptyset}\right) = \left(1 + \frac{g\bar{\gamma}_J}{sin^2\emptyset}\right)^{-1}. \tag{17}$$

b) For Rician with factor K,

$$M_{\gamma_J}\left(\frac{-g}{sin^2\emptyset}\right) = \frac{(1+K)sin^2\emptyset}{(1+K)sin^2\emptyset+g\bar{\gamma}_J} \exp\left[\frac{-Kg\bar{\gamma}_J}{(1+K)sin^2\emptyset+g\bar{\gamma}_J}\right]. \tag{18}$$

c) For Nakagami-*m* fading,

$$M_{\gamma_J}\left(\frac{-g}{sin^2\emptyset}\right) = \left(1 + \frac{g\bar{\gamma}_J}{msin^2\emptyset}\right)^{-m}. \tag{19}$$

Our results are applicable for other modulations by modifying (12) and other fading environments by finding the corresponding MGF for the other fading. For example, the exact SER of a rectangular MQAM modulation can be written as

$$P_s(E|\gamma) = 1 - \left(1 - \frac{2\left(\sqrt{M}-1\right)}{\sqrt{M}} Q\left(\sqrt{3\gamma/(M-1)}\right)\right)^2$$

$$= 1 - \left(1 - \frac{2\left(\sqrt{M}-1\right)}{\sqrt{M}} \frac{1}{\pi}\int_0^{\pi/2} exp\left[\frac{-3\gamma/(M-1)}{2sin^2\emptyset}\right] d\emptyset\right)^2 \tag{20}$$

where γ is the instantaneous SNR under fading but the averaged SNR over all possible M-ary constellation points for a given fading coefficient. Substituting (20) into (12), we can find the exact SER of the FH MQAM under PBTJ plus Rician fading as we have done for the FH MPSK. Therefore, we present only the Rician fading and MPSK modulation case in the remainder of this paper.

In (16), we need to calculate the average SJNR $\bar{\gamma}_J$ over the Rician fading under the PBTJ condition as

$$\bar{\gamma}_J = E_{|h_1|^2}\left[\frac{(|h_1|)^2}{\left(\frac{1}{\beta E_S/N_J}+\frac{1}{E_S/N_0}\right)}\right] = \frac{1}{\left(\frac{1}{\beta E_S/N_J}+\frac{1}{E_S/N_0}\right)} E_{|h_1|^2}[|h_1|^2]. \tag{21}$$

The $E_{|h_1|^2}[|h_1|^2]$ can be computed using [23] as

$$E_{|h_1|^2}[|h_1|^2] = \sigma\sqrt{\pi/2}\, L_{1/2}(-s^2/2\sigma^2) = \sigma\sqrt{\pi/2}\, L_{1/2}(-K) \tag{22}$$

where $2\sigma^2$ is the non-line-of-sight (NLOS) component power, s^2 is the LOS component power, and $K = s^2/\,2\sigma^2$ is the ratio of the line-of-sight (LOS) over NLOS component power called the Rician factor. Here, the $L_{1/2}(x)$ is the Laguerre polynomial, written as

$$L_{1/2}(x) = e^{x/2}\left[(1-x)I_0\left(\frac{-x}{2}\right) - xI_1\left(\frac{-x}{2}\right)\right] \tag{23}$$

where $I_0(x)$ and $I_1(x)$ are the zeroth order and the first-order modified Bessel function of the first kind, respectively. Assume $\sigma^2 = 1$ without of loss of generality. Hence,

$$\begin{aligned} E_{|h_1|^2}[|h_1|^2] &= \sigma\sqrt{\pi/2}\, L_{1/2}(-s^2/2\sigma^2) = \sqrt{\pi/2}\, L_{1/2}(-K) \\ &= \sqrt{\pi/2}\, e^{-K/2}\left[(1+K)I_0\left(\frac{K}{2}\right) + KI_1\left(\frac{K}{2}\right)\right]. \end{aligned} \tag{24}$$

$$\bar{\gamma}_J = \frac{1}{\left(\frac{1}{\beta E_S/N_J} + \frac{1}{E_S/N_0}\right)}\sqrt{\pi/2}\, e^{-K/2}\left[(1+K)I_0\left(\frac{K}{2}\right) + KI_1\left(\frac{K}{2}\right)\right]. \tag{25}$$

Substituting $\bar{\gamma}_J$ into (16), we can find an exact conditional SER of the FH MPSK given a PBTJ condition.

We repeat (16) to (25) to obtain the conditional average SER under no-jamming as

$$\begin{aligned} E_{\gamma_N}\left[P_s\left(E\middle|\gamma_J, J=0\right)\right] &= \int_0^\infty P_s(E|\gamma_N, J=0)\, p_{\gamma_N}(\gamma_N)\, d\gamma_N \\ &= \frac{1}{\pi}\int_0^{(M-1)\pi/M} \frac{(1+K)}{(1+K)+\frac{g}{\sin^2\emptyset}\bar{\gamma}_N} \exp\left[\frac{-K\frac{g}{\sin^2\emptyset}\bar{\gamma}_N}{(1+K)+\frac{g}{\sin^2\emptyset}\bar{\gamma}_N}\right] d\emptyset \end{aligned} \tag{26}$$

where

$$\bar{\gamma}_N = \frac{E_S}{N_0}\sqrt{\frac{\pi}{2}}e^{-K/2}\left[(1+K)I_0\left(\frac{K}{2}\right) + KI_1\left(\frac{K}{2}\right)\right]. \tag{27}$$

Therefore, the overall averaged exact SER of the FH MPSK under PBTJ and Rician fading can be written using (14), (16), and (25)–(27) as

$$\begin{aligned} \bar{P}_s(E|\beta) = {} & \frac{1}{\pi}\int_0^{(M-1)\pi/M} \frac{(1+K)}{(1+K)+\frac{g}{\sin^2\emptyset}\bar{\gamma}_J} \exp\left[\frac{-K\frac{g}{\sin^2\emptyset}\bar{\gamma}_J}{(1+K)+\frac{g}{\sin^2\emptyset}\bar{\gamma}_J}\right] d\emptyset \cdot \beta \\ & + \frac{1}{\pi}\int_0^{(M-1)\pi/M} \frac{(1+K)}{(1+K)+\frac{g}{\sin^2\emptyset}\bar{\gamma}_N} \exp\left[\frac{-K\frac{g}{\sin^2\emptyset}\bar{\gamma}_N}{(1+K)+\frac{g}{\sin^2\emptyset}\bar{\gamma}_N}\right] d\emptyset \cdot (1-\beta). \end{aligned} \tag{28}$$

The average SER for a given jamming fraction ratio β can be rewritten by substituting (25) and (27) into (28) as

$$\bar{P}_s(E|\beta) = \frac{1}{\pi}\int_0^{(M-1)\pi/M} \left[\frac{\beta(1+K)}{(1+K)+\frac{g}{\sin^2\emptyset}\frac{1}{\left(\frac{1}{\beta E_S/N_J}+\frac{1}{E_S/N_0}\right)}\sqrt{\pi/2}e^{-\frac{K}{2}}\left[(1+K)I_0\left(\frac{K}{2}\right)+KI_1\left(\frac{K}{2}\right)\right]}\right.$$

$$\cdot \exp\left(\frac{\frac{-K\frac{g}{\sin^2\emptyset}}{\left(\frac{1}{\beta E_S/N_J}+\frac{1}{E_S/N_0}\right)}\sqrt{\pi/2}e^{-\frac{K}{2}}\left[(1+K)I_0\left(\frac{K}{2}\right)+KI_1\left(\frac{K}{2}\right)\right]}{(1+K)+\frac{g}{\sin^2\emptyset}\frac{1}{\left(\frac{1}{\beta E_S/N_J}+\frac{1}{E_S/N_0}\right)}\sqrt{\pi/2}e^{-\frac{K}{2}}\left[(1+K)I_0\left(\frac{K}{2}\right)+KI_1\left(\frac{K}{2}\right)\right]}\right)\Bigg] d\emptyset$$

$$+\frac{1}{\pi}\int_0^{(M-1)\pi/M}\frac{(1-\beta)(1+K)}{(1+K)+\frac{g}{\sin^2\emptyset}\bar{\gamma}_N}\exp\left[\frac{-K\frac{g}{\sin^2\emptyset}\bar{\gamma}_N}{(1+K)+\frac{g}{\sin^2\emptyset}\bar{\gamma}_N}\right]d\emptyset. \quad (29)$$

The averaged bit error rate of the FH MPSK under PBTJ and Rician fading for a given jamming fraction ratio β can be obtained using (29) as

$$\bar{P}_b(E|\beta)=\frac{1}{log_2(M)}\bar{P}_s(E|\beta). \quad (30)$$

Here, we assume Gray encoding so that the neighbor signal constellations are only one bit different from the desired symbol constellation point.

For a special case, consider only AWGN and PBTJ. Then, the Rician factor K becomes ∞. So, the exact SER of the FH MPSK under AWGN and PBTJ can be written as

$$P_s(E|\beta)=\frac{1}{\pi}\int_0^{(M-1)\pi/M}\exp\left[-\frac{g}{\sin^2\emptyset}\gamma_N\right]d\emptyset\cdot(1-\beta)+\frac{1}{\pi}\int_0^{(M-1)\pi/M}\exp\left[-\frac{g}{\sin^2\emptyset}\gamma_J\right]d\emptyset\cdot\beta \quad (31)$$

where SNR $\gamma_N=E_S/N_0$ and SJNR $\gamma_J=\frac{1}{\left(\frac{1}{\beta E_S/N_J}+\frac{1}{E_S/N_0}\right)}$ from (10). Thus, the first and second terms of (31) represent the exact SER when the signal is not jammed with probability $(1-\beta)$ and jammed with probability β, respectively.

IV. Optimal Tone-Jamming Fraction

The optimum jamming fraction β, which maximizes the average conditional SER $\bar{P}_s(E|\beta)$ can be numerically found by taking the derivative of (29) with respect to β for a given set of parameters, such as E_S/N_J, E_S/N_0, and M, and Rician fading factor K. The optimum β should satisfy the following equation:

$$\frac{1}{\pi}\int_0^{(M-1)\pi/M}\frac{(1+K)}{(1+K)+\frac{g}{\sin^2\emptyset}\bar{\gamma}_N}\exp\left[\frac{-K\frac{g}{\sin^2\emptyset}\bar{\gamma}_N}{(1+K)+\frac{g}{\sin^2\emptyset}\bar{\gamma}_N}\right]d\emptyset$$

$$=\frac{1}{\pi}\int_0^{(M-1)\pi/M}\left[\frac{-g\bar{\gamma}_J N_J\sin^2\emptyset(1+K)}{\beta(1+K)\sin^2\emptyset+g\bar{\gamma}_J\beta}+\exp\left(\frac{-Kg\gamma_J}{(1+K)\sin^2\emptyset+g\gamma_J}\right)\right.$$

$$\left.\cdot\frac{g\bar{\gamma}_J\cdot\sin^2\emptyset\cdot(1+K)\left(N_0K+\frac{\beta-K}{\beta}\right)+(1+K)^2\cdot\sin^4\emptyset\cdot(N_0\beta+N_J)}{g\bar{\gamma}_J+(1+K)\cdot\sin^2\emptyset}\right]d\emptyset. \quad (32)$$

The left term of (32) is the derivative of the second term on the right-hand side of (29), and the right term of (32) is the derivative of the first term on the right-hand side of (29). Using Newton's method, we can solve the optimum beta using (32).

V. Numerical Results

Figs. 3 to 8 show BER versus E_s/N_0 with PBTJ fraction β in percentile as a parameter for a given $E_s/N_J = 5\ dB$ or $10\ dB$, given Rician factor $K = 0.9$ or 0.1, and given QPSK modulation. Figs. 9 to 12 show SER versus E_s/N_0 with modulation as a parameter for a given $E_s/N_J = 10\ dB$ or $20\ dB$, given Rician factor $K = 0$ or 0.9, and given PBTJ fraction $\beta = 0.9$ or 0.1. Table 1 lists the parameters used for numerical results shown in Figs. 3 to 12. Here, $p_J = Pr(Tone\ Jammed\ by\ PBTJ) = \beta$. Equations (29) and (30) are used.

TABLE I. Parameters Used For BER Analysis.

Fig.	***Rician Factor (K)***	***Modulation***	$\boldsymbol{E_S/N_J}$ ***(dB)***	$\boldsymbol{\beta = p_J}$
3	0.1	QPSK	10	0 to 0.9
4	0.1	QPSK	5	0 to 0.9
5	0.5	QPSK	10	0 to 0.9
6	0.5	QPSK	5	0 to 0.9
7	0.9	QPSK	10	0 to 0.9
8	0.9	QPSK	5	0 to 0.9
9	0	QPSK to 64PSK	10	0.9
10	0	QPSK to 64PSK	20	0.9
11	0.9	QPSK to 64PSK	10	0.1
12	0.9	QPSK to 64PSK	20	0.1

Figs. 13 and 14 show SER versus PBTJ fraction β with a modulation as a parameter for a given $E_s/N_J = 10\ dB$ or $20\ dB$, for a given $E_s/N_0 = 10\ dB$, a given Rician factor $K = 0.1$ or 0.9, and BPSK modulation. Table II lists the parameters for the BER shown in Figs. 13 and 14 versus PBTJ fraction β, using (29) and (30).

Fig. 15 also shows BER versus PBTJ jamming fraction β with an E_s/N_J as a parameter for a given $E_s/N_0 = 30\ dB$, a given Rician factor $K = 0.1$, and BPSK modulation, using (29) and (30).

TABLE II. PARAMETERS USED FOR BER PLOTS VS. TONE-JAMMING FRACTION.

Fig.	***Rician Factor (K)***	***Modulation***	E_S/N_J ***(dB)***	E_S/N_0 ***(dB)***
13	0.1	QPSK	10	10
	0.1	8-PSK	10	10
	0.1	16-PSK	10	10
	0.1	32-PSK	10	10
	0.1	64-PSK	10	10
14	0.9	QPSK	20	10
	0.9	8-PSK	20	10
	0.9	16-PSK	20	10
	0.9	32-PSK	20	10
	0.9	64-PSK	20	10

Figs. 16 to 24 show the corresponding results to Rician fading of a strong LOS component case with $K = 5$, using (29) and (30). Fig. 25 also shows BER versus PBTJ jamming fraction β with E_S/N_J as a parameter, using (31) for no fading but under AWGN and PBTJ, for a given $E_b/N_0 = 10\ dB$ and for BPSK modulation.

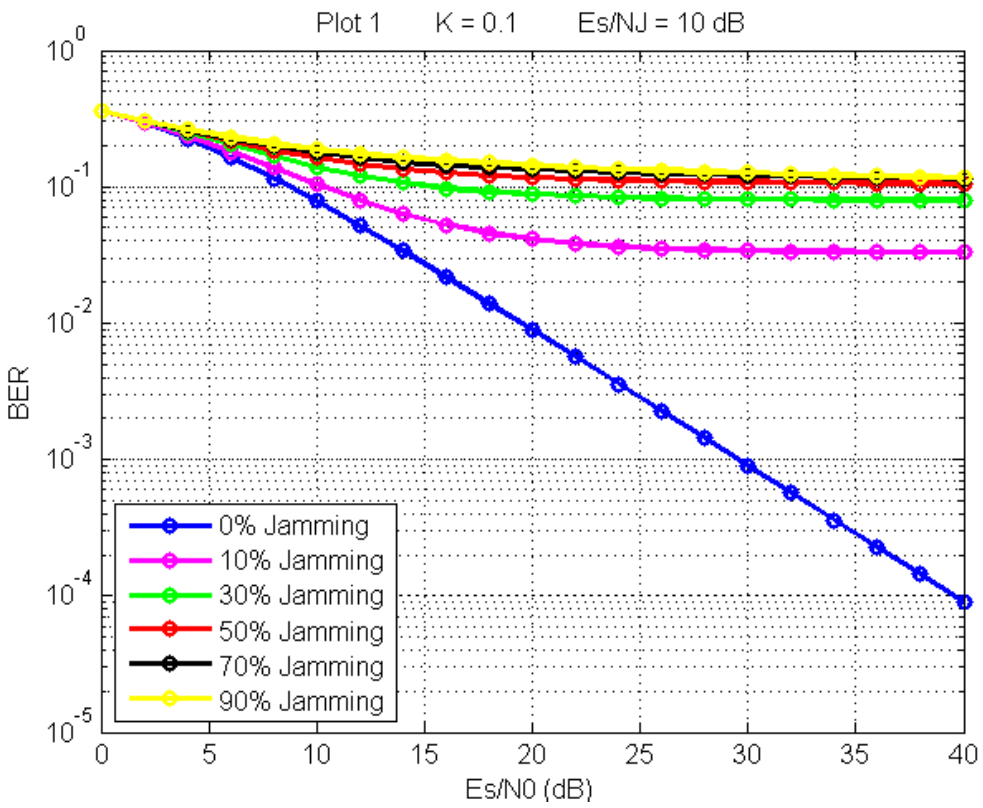

Fig. 3. BER versus E_s/N_0 in dB for QPSK under Rician of factor $K = 0.1$, $E_s/N_J = 10\ dB$ with PBTJ fraction β in percentile as a parameter.

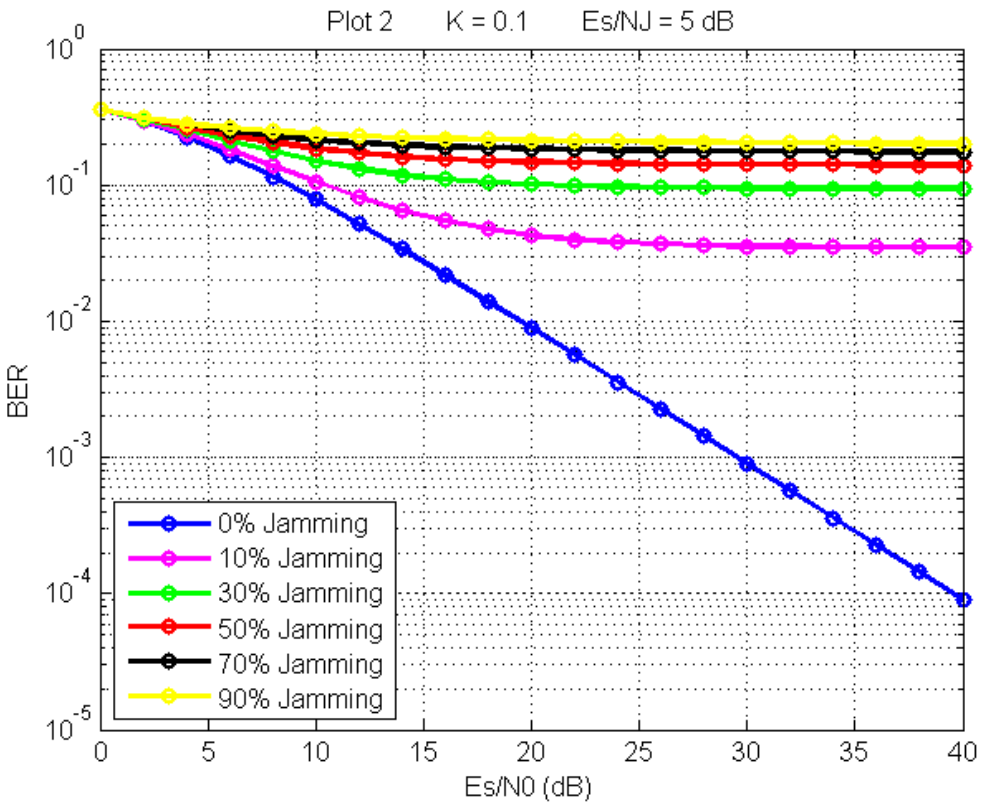

Fig. 4. BER versus E_s/N_0 in dB for QPSK under Rician of factor $K = 0.1$, $E_s/N_J = 5\ dB$ with PBTJ fraction β in percentile as a parameter.

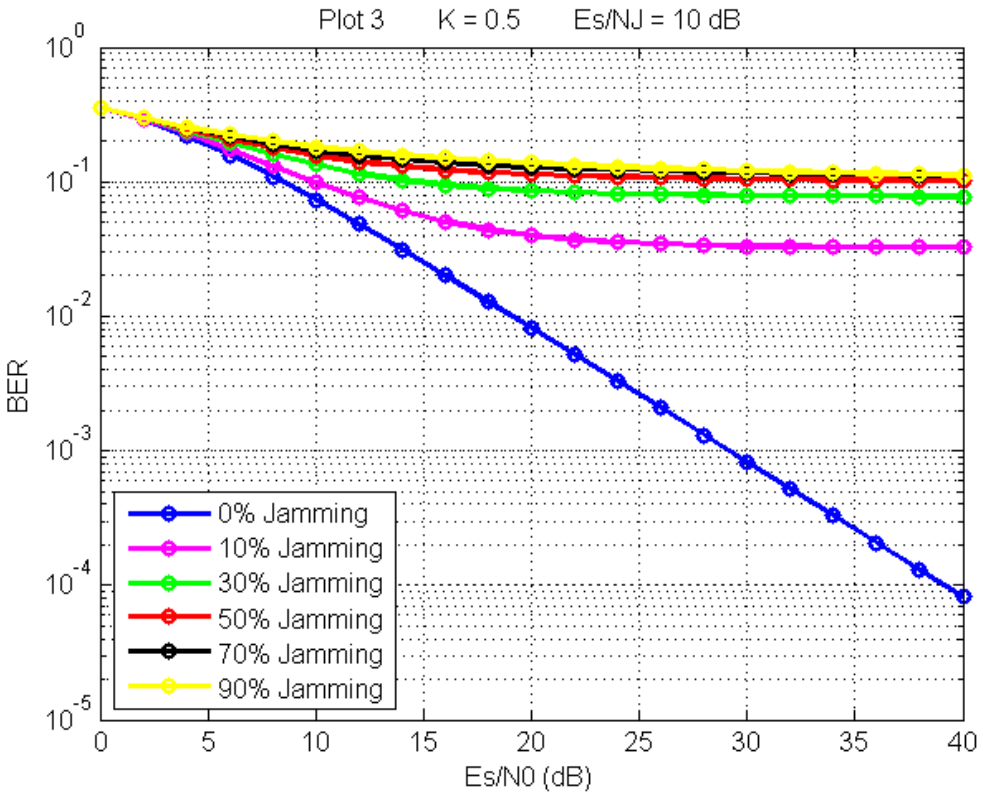

Fig. 5. BER versus E_s/N_0 in dB for QPSK under Rician of factor $K = 0.5$, $E_s/N_J = 10\ dB$ with PBTJ fraction β in percentile as a parameter.

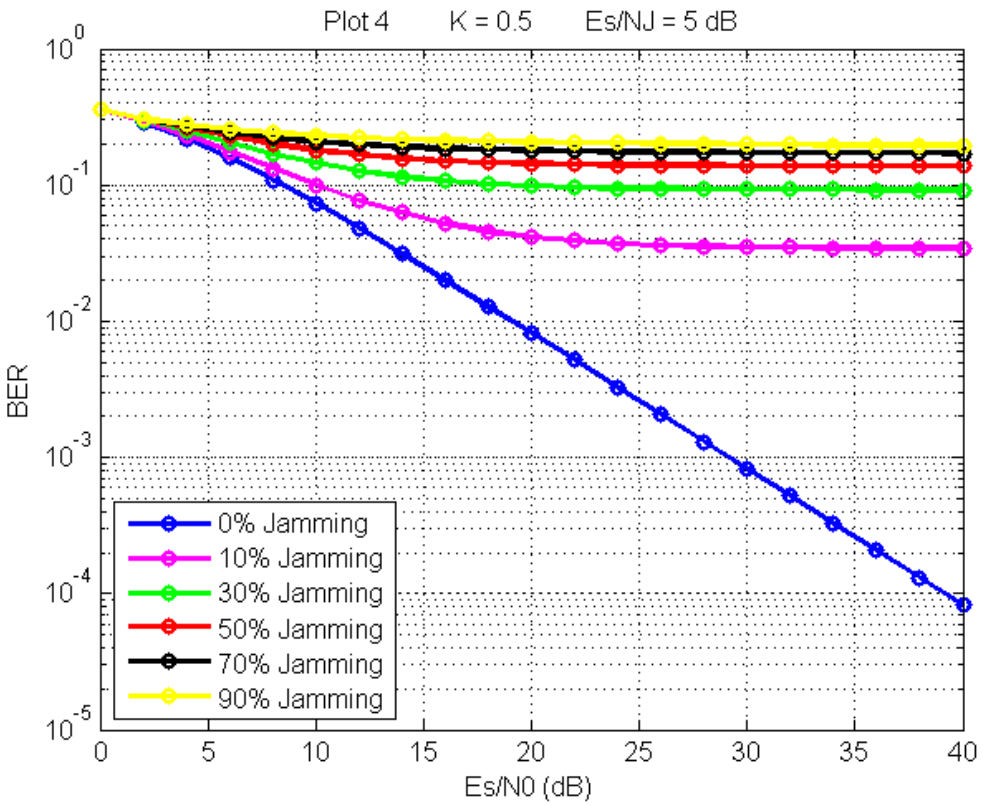

Fig. 6. BER versus E_s/N_0 in dB for QPSK under Rician of factor $K = 0.5$, $E_s/N_J = 5\ dB$ with PBTJ fraction β in percentile as a parameter.

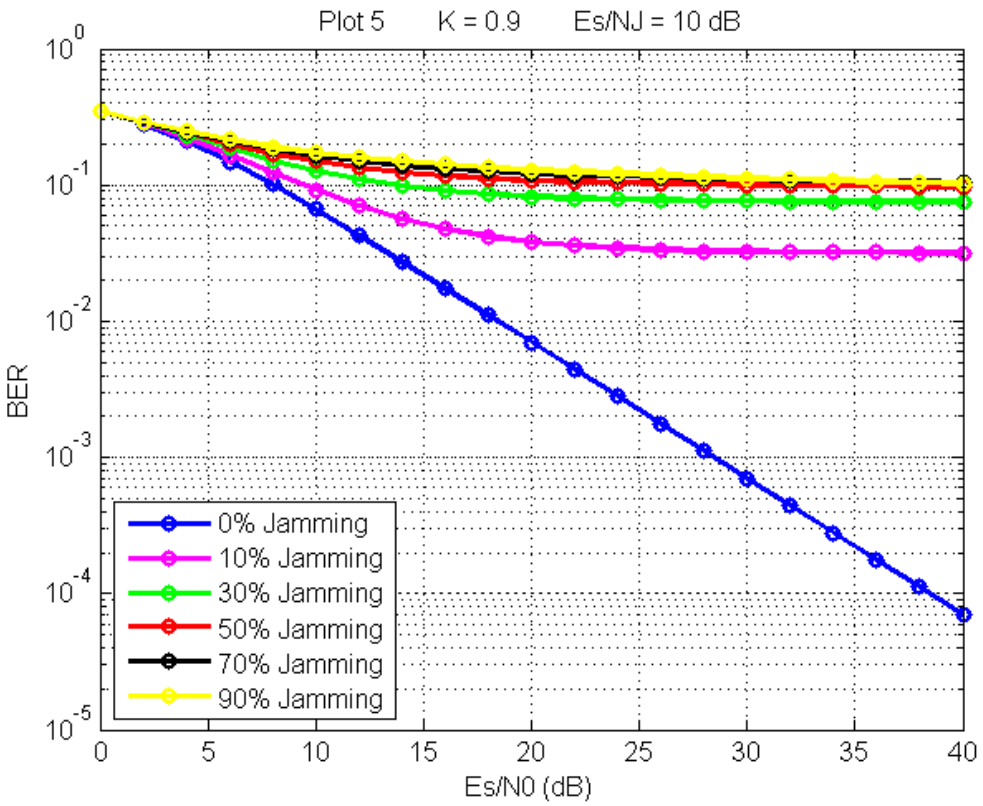

Fig. 7. BER versus E_s/N_0 in dB for QPSK under Rician of factor $K = 0.9$, $E_s/N_J = 10\ dB$ with PBTJ fraction β in percentile as a parameter.

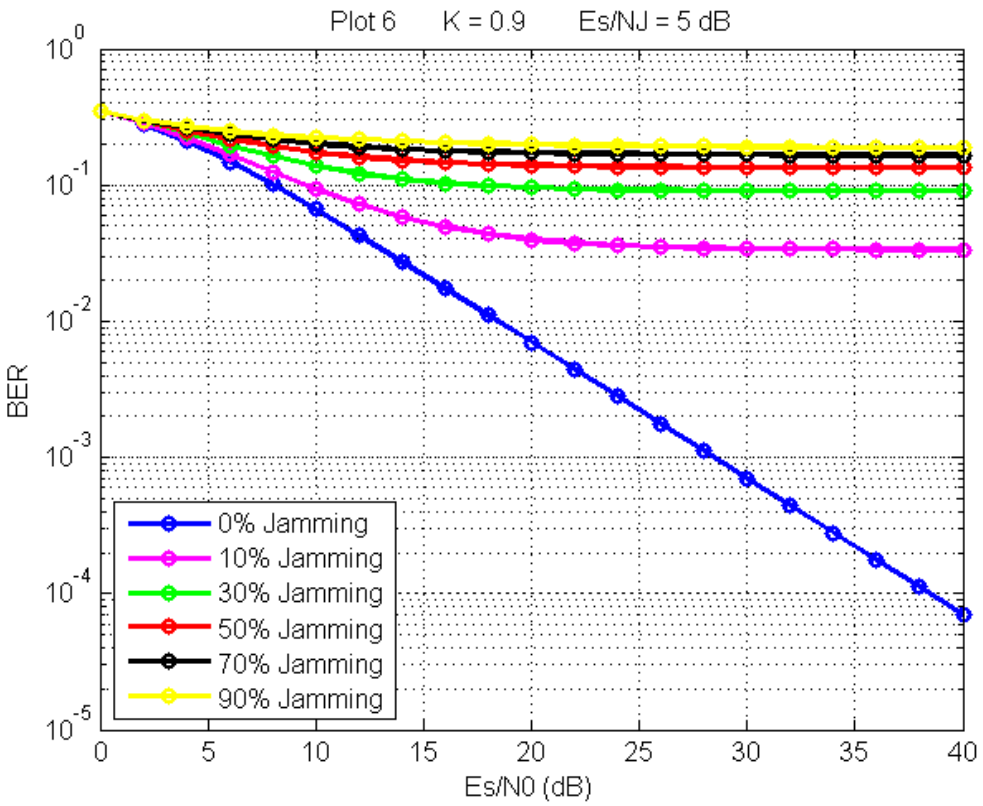

Fig. 8. BER versus E_s/N_0 in dB for QPSK under Rician of factor $K = 0.9$, $E_s/N_J = 5\ dB$ with PBTJ fraction β in percentile as a parameter.

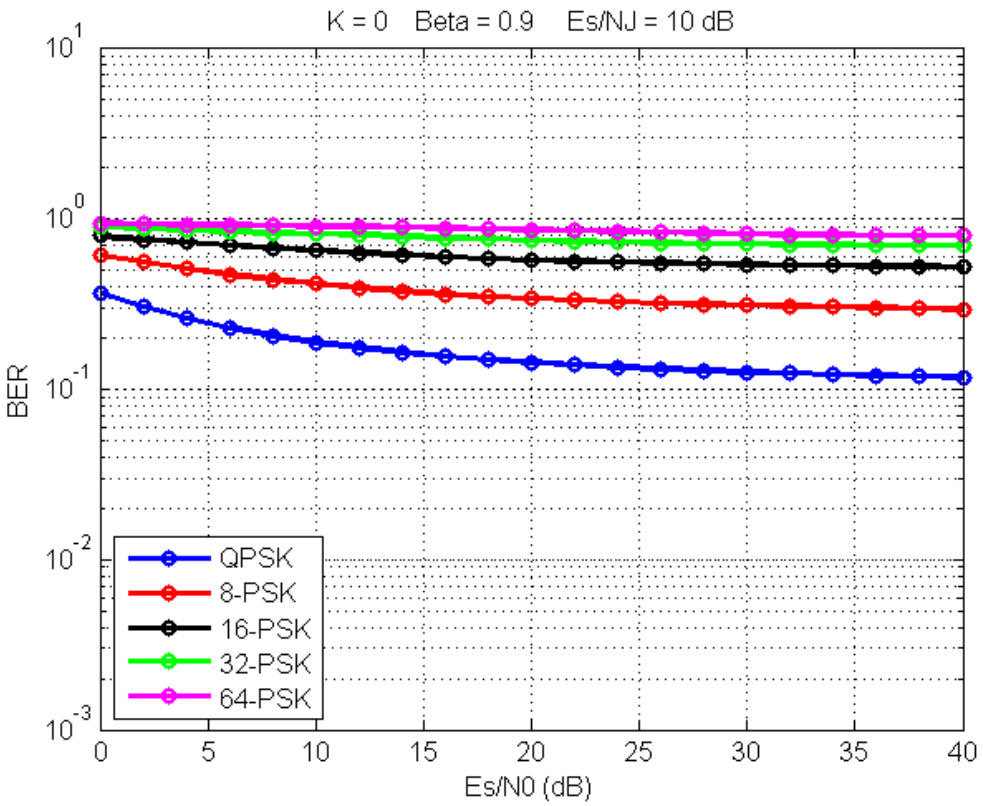

Fig. 9. BER versus E_s/N_0 in dB for QPSK under Rician of factor $K = 0$ (i.e., Rayleigh fading and no LOS), $E_s/N_J = 10\ dB$, PBTJ fraction $\beta = 0.9$ with MPSK as a parameter.

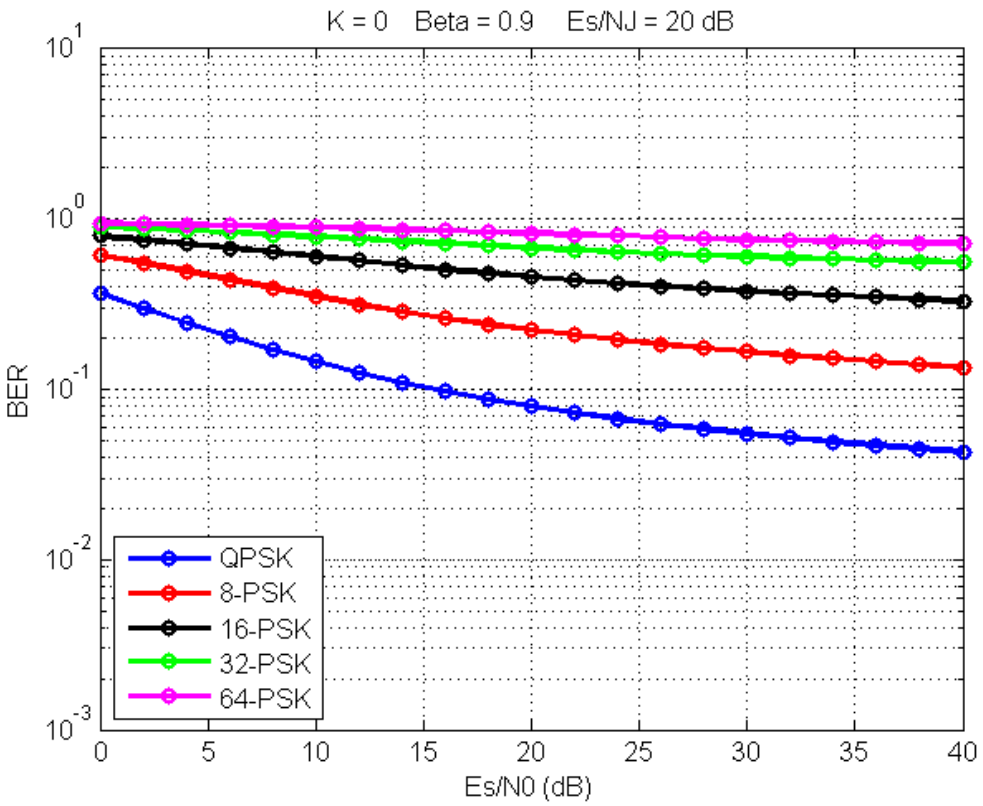

Fig. 10. BER versus E_s/N_0 in dB for QPSK under Rician of factor $K = 0$ (i.e., Rayleigh fading and no LOS), $E_s/N_J = 20\ dB$, PBTJ fraction $\beta = 0.9$ with MPSK as a parameter.

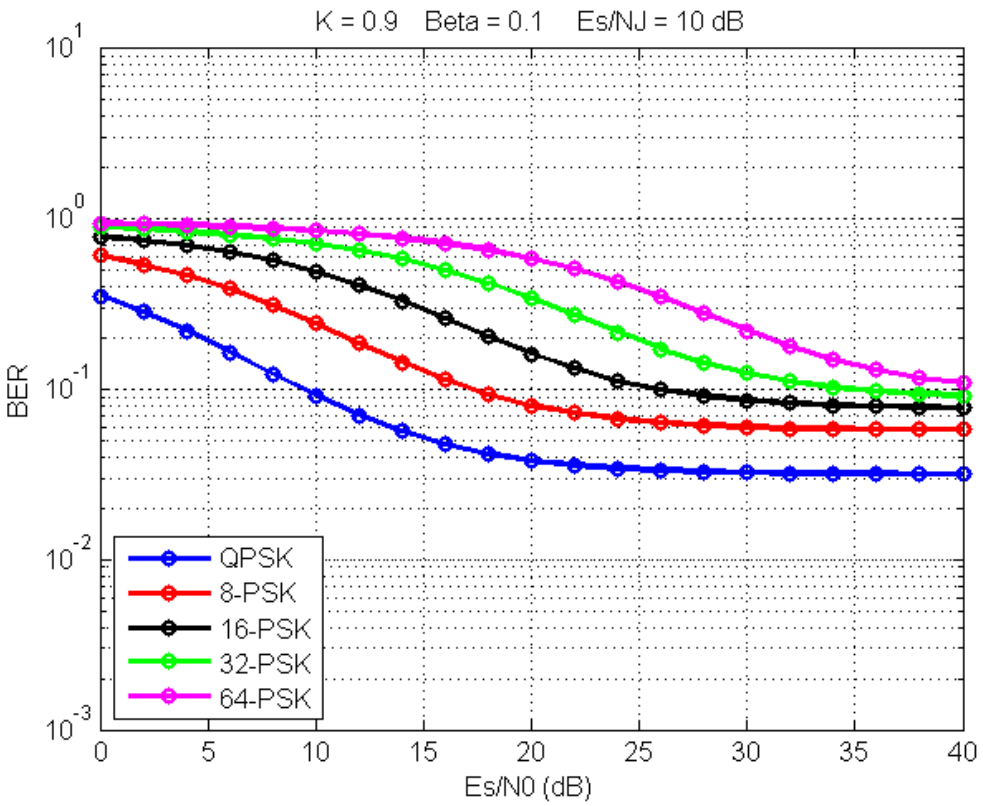

Fig. 11. BER versus E_s/N_0 in dB for QPSK under Rician of factor $K = 0.9$, $E_s/N_J = 10\ dB$, PBTJ fraction $\beta = 0.1$ with MPSK as a parameter.

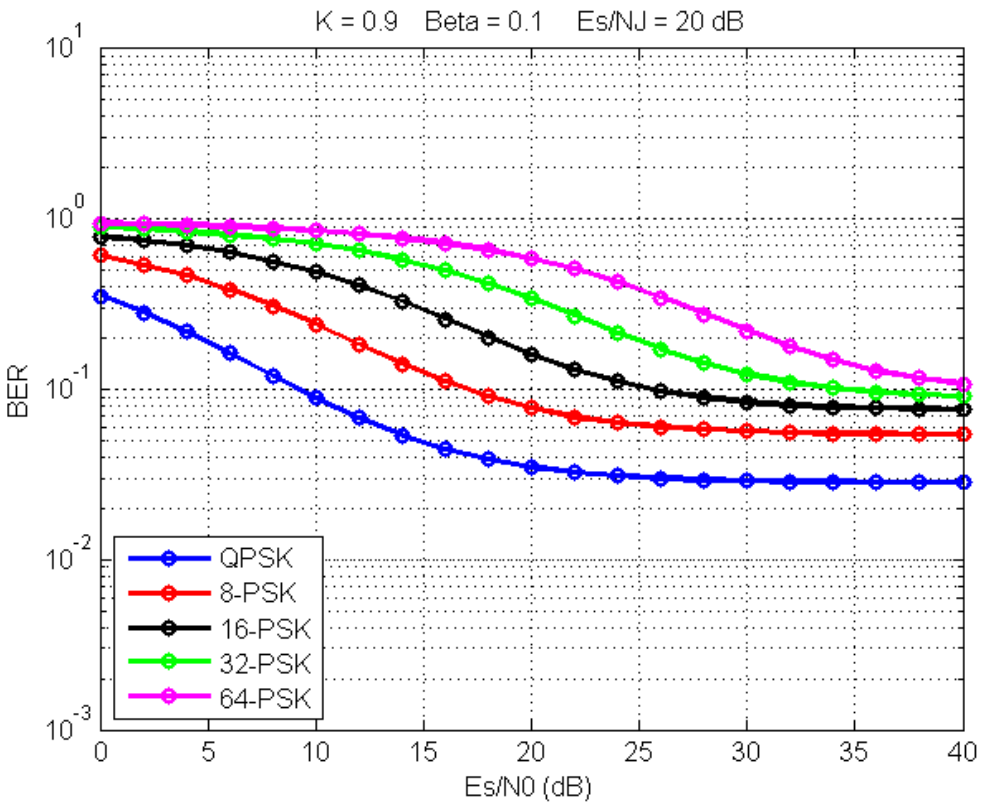

Fig. 12. BER versus E_s/N_0 in dB for QPSK under Rician of factor $K = 0.9$, $E_s/N_J = 20\ dB$, PBTJ fraction $\beta = 0.1$ with MPSK as a parameter.

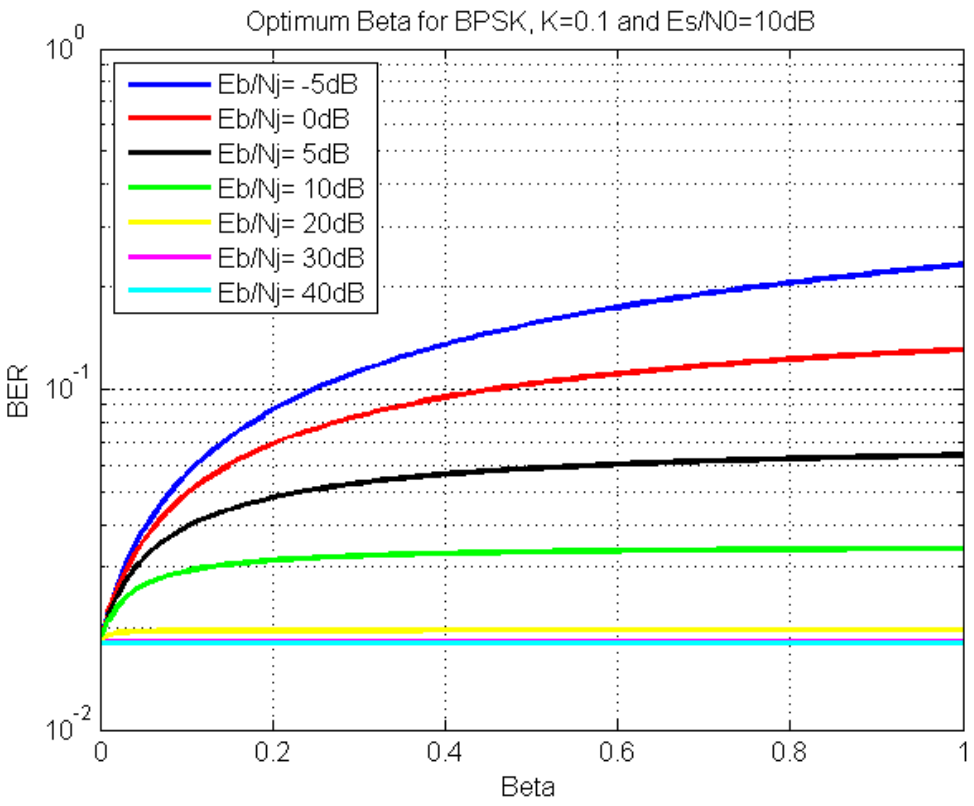

Fig. 13. BER versus PBTJ fraction β for BPSK under Rician fading of factor $K = 0.1$, $E_b/N_0 = 10\ dB$ with E_b/N_J as a parameter in dB.

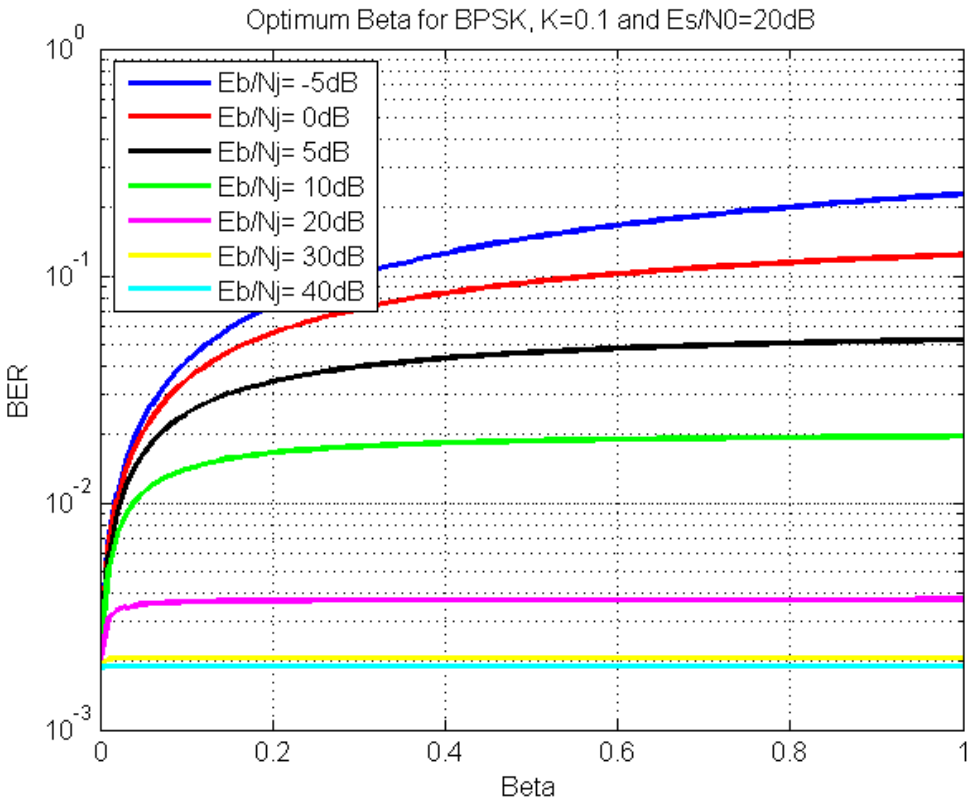

Fig. 14. BER versus PBTJ fraction β for BPSK under Rician fading of factor $K = 0.1,\ E_b/N_0 = 20\ dB$ with E_b/N_J as a parameter in dB.

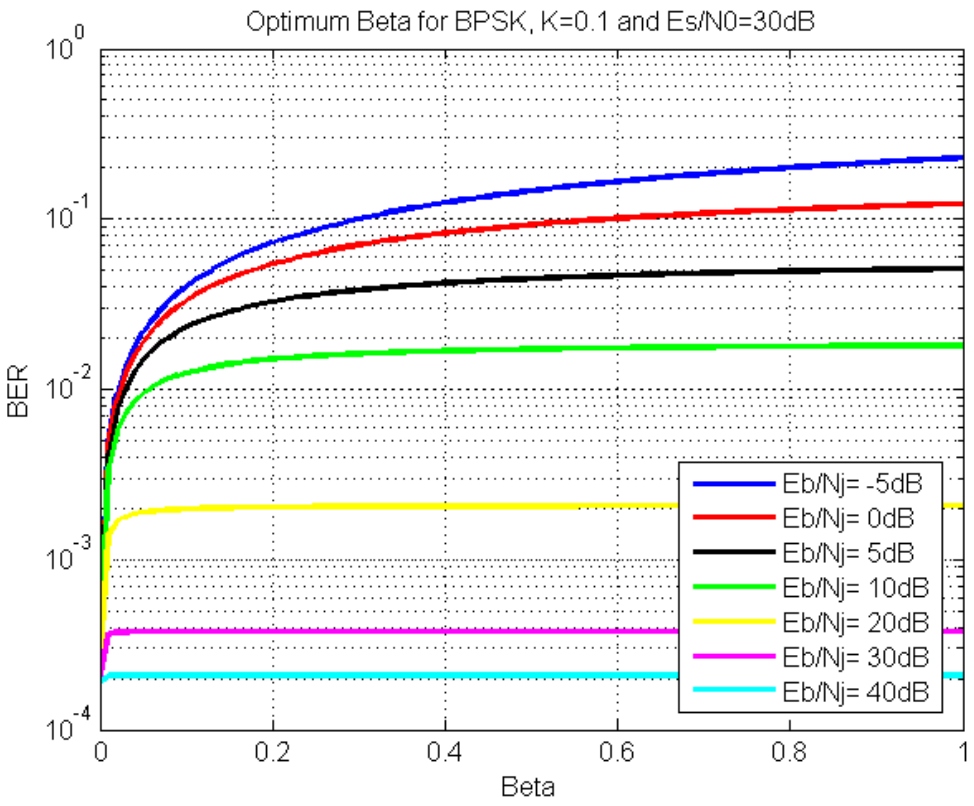

Fig. 15. BER versus PBTJ fraction β for BPSK under Rician fading of factor $K = 0.1$, $E_b/N_0 = 30\ dB$ with E_b/N_J as a parameter in dB.

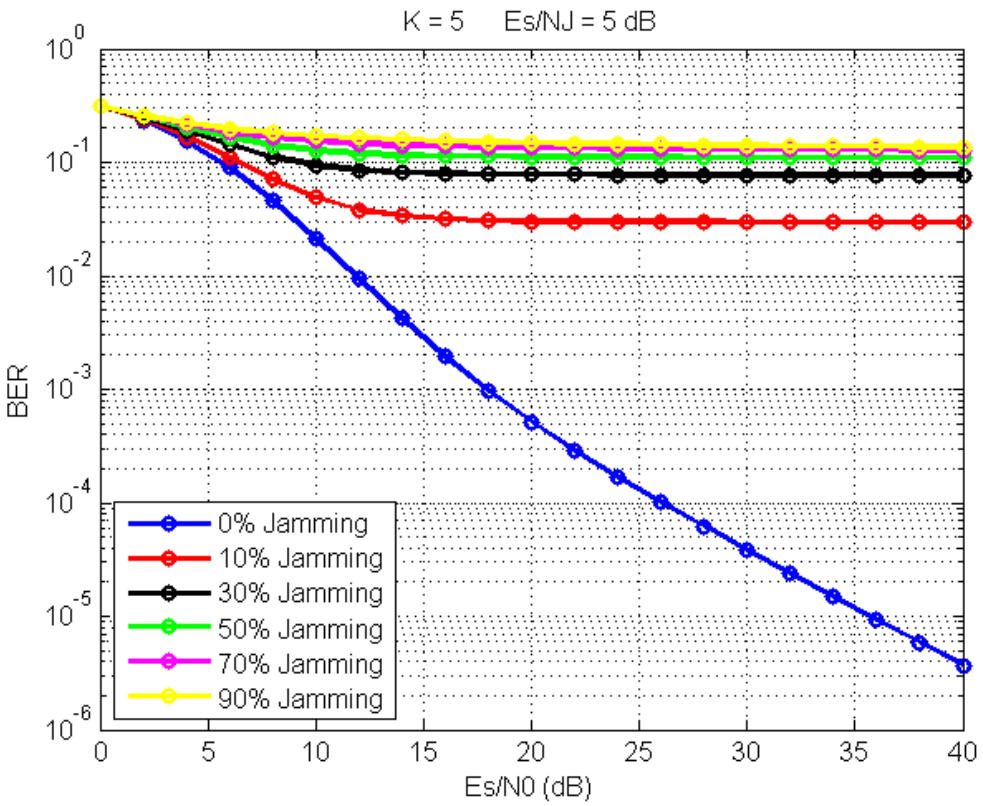

Fig. 16. BER versus E_s/N_0 in dB for QPSK under Rician of factor $K = 5$, $E_s/N_J = 5\ dB$ with PBTJ fraction β in percentile as a parameter.

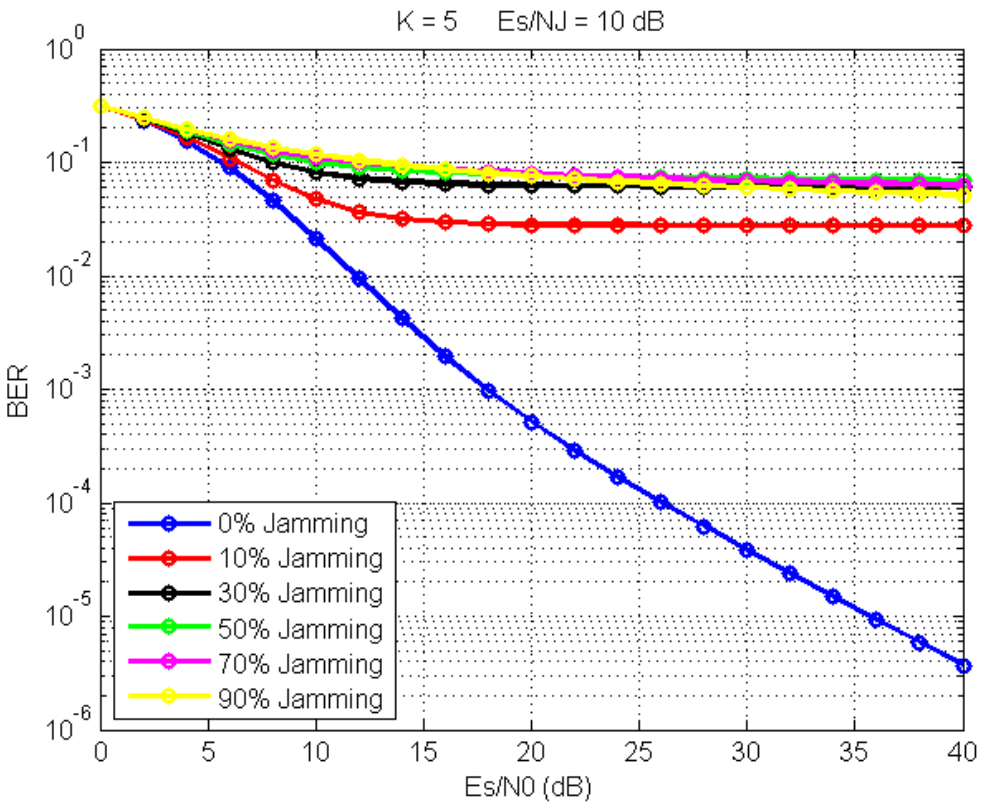

Fig. 17. BER versus E_s/N_0 in dB for QPSK under Rician of factor $K = 5$, $E_s/N_J = 10\ dB$ with PBTJ fraction β in percentile as a parameter.

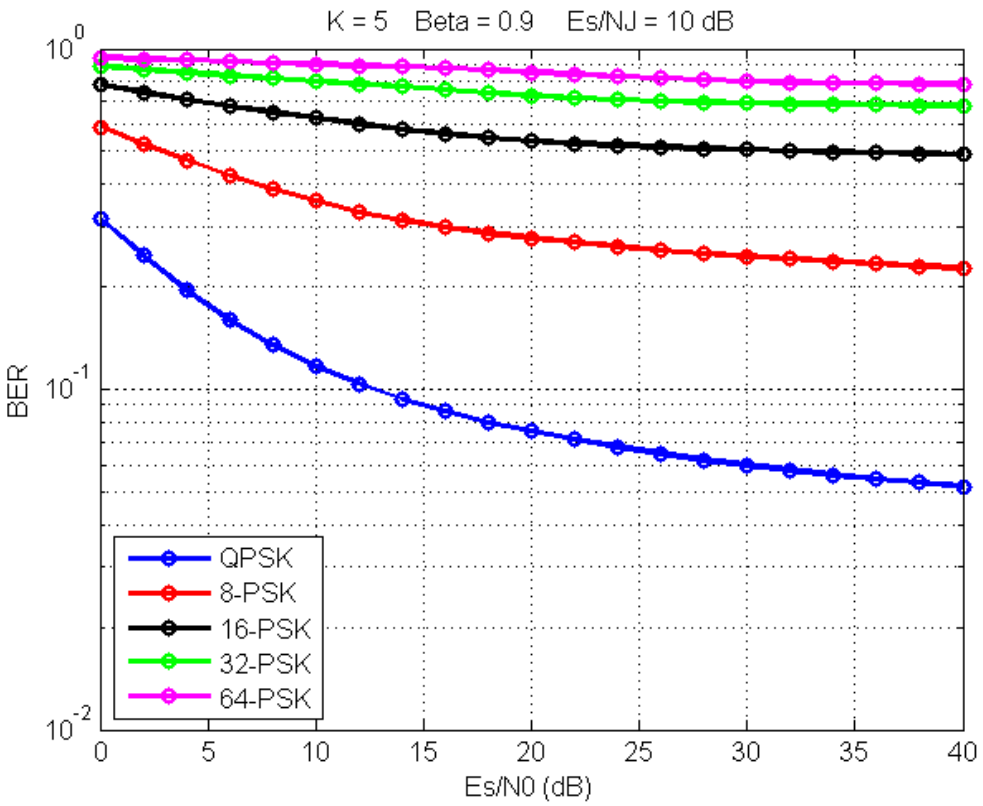

Fig. 18. BER versus E_s/N_0 in dB for QPSK under Rician of factor $K = 5$, $E_s/N_J = 10\ dB$, PBTJ fraction $\beta = 0.9$ with MPSK as a parameter.

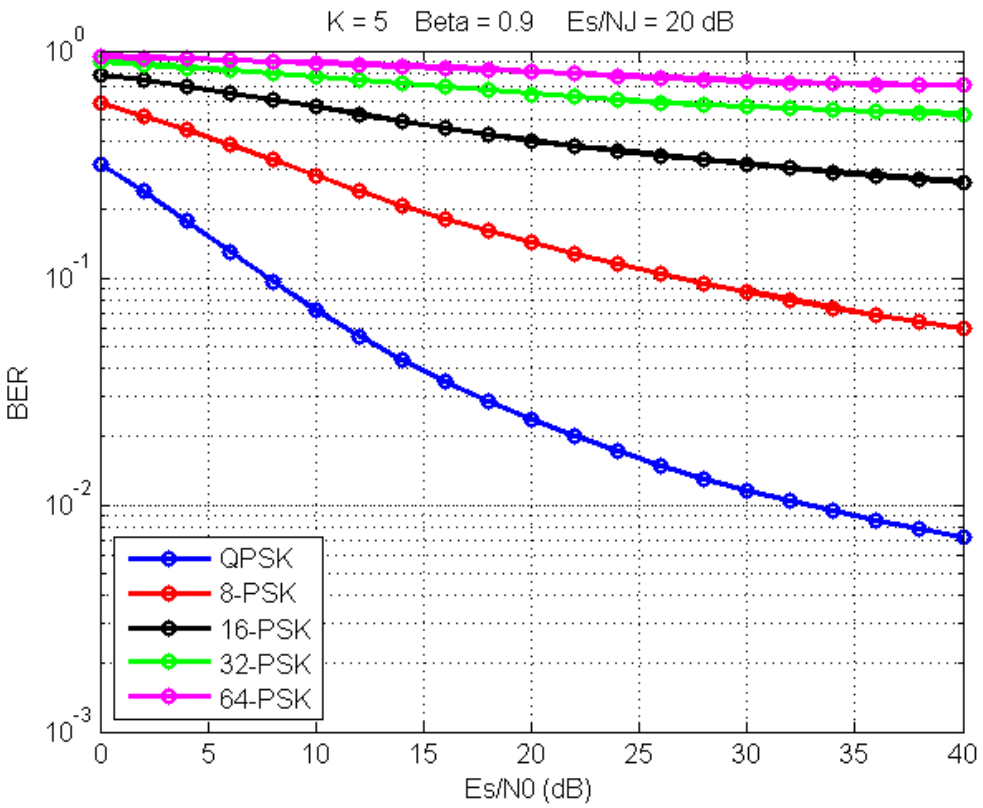

Fig. 19. BER versus E_s/N_0 in dB for QPSK under Rician of factor $K = 5$, $E_s/N_J = 20\ dB$, PBTJ fraction $\beta = 0.9$ with MPSK as a parameter.

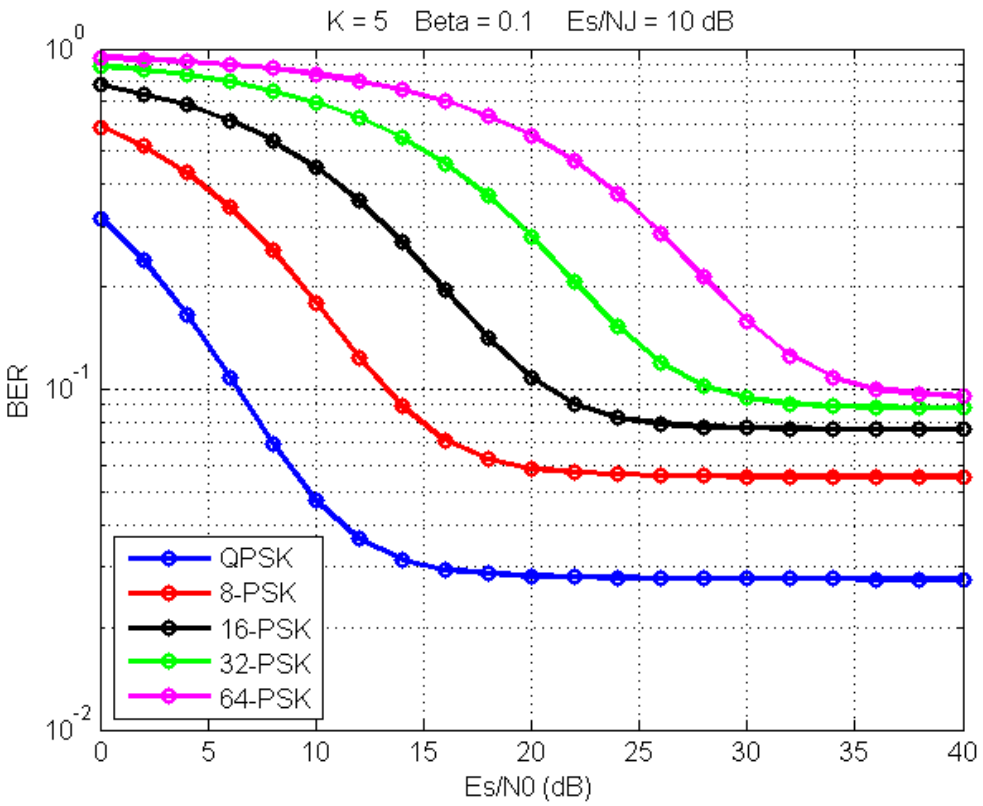

Fig. 20. BER versus E_s/N_0 in dB for QPSK under Rician of factor $K = 5$, $E_s/N_J = 10\ dB$, PBTJ fraction $\beta = 0.1$ with MPSK as a parameter.

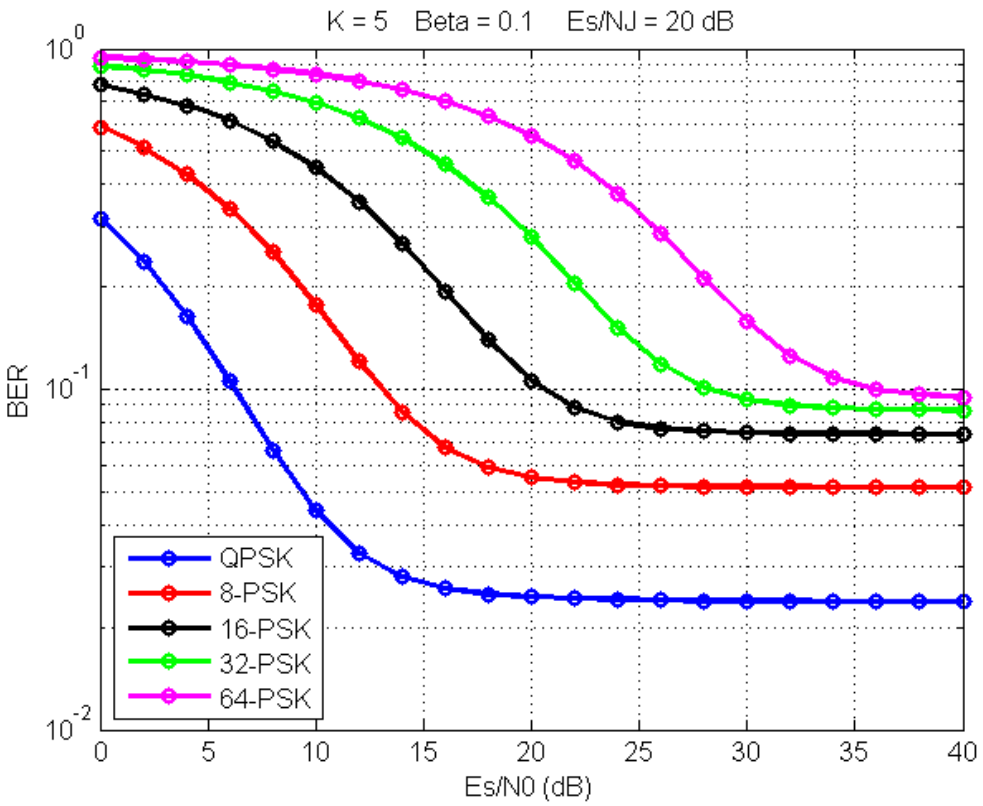

Fig. 21. BER versus E_s/N_0 in dB for QPSK under Rician of factor $K = 5$, $E_s/N_J = 20\ dB$, PBTJ fraction $\beta = 0.1$ with MPSK as a parameter.

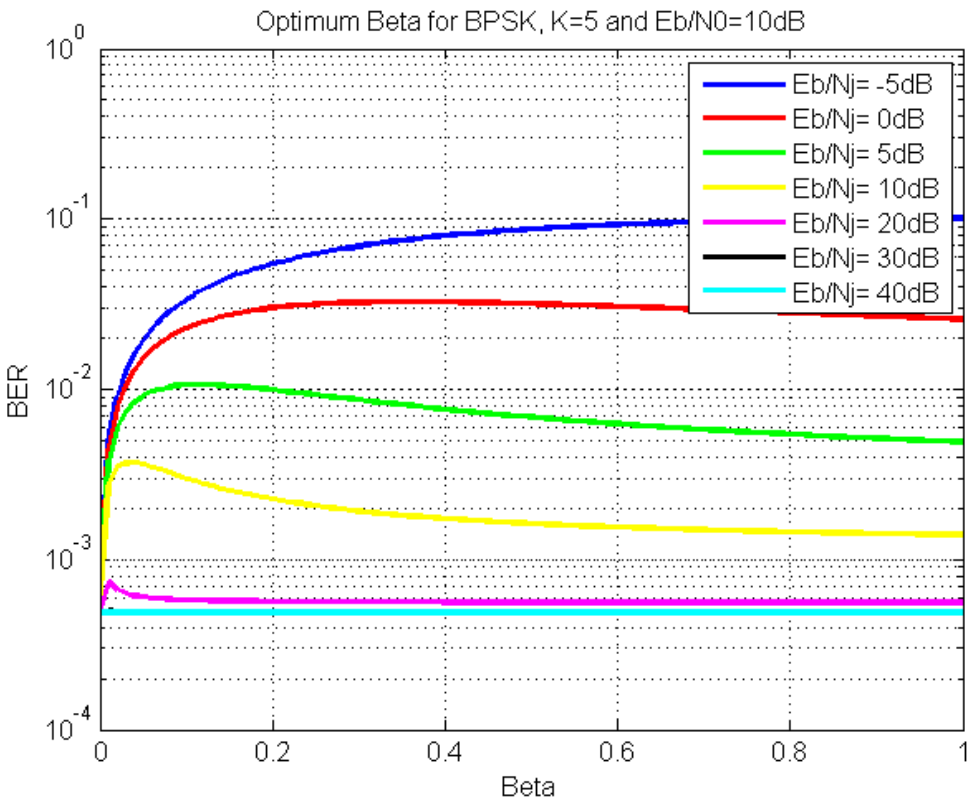

Fig. 22. BER versus PBTJ fraction β for BPSK under Rician fading of factor $K = 5$, $E_b/N_0 = 10\ dB$ with E_b/N_J as a parameter in dB.

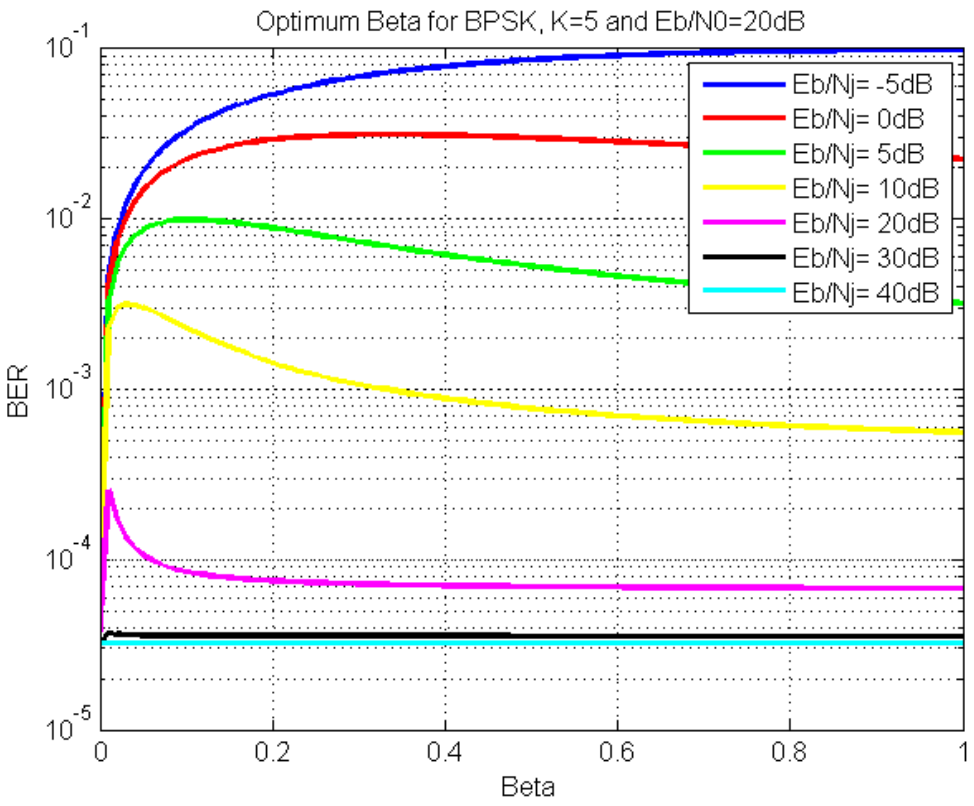

Fig. 23. BER versus PBTJ fraction β for BPSK under Rician fading of factor $K = 5$, $E_b/N_0 = 20\ dB$ with E_b/N_J as a parameter in dB.

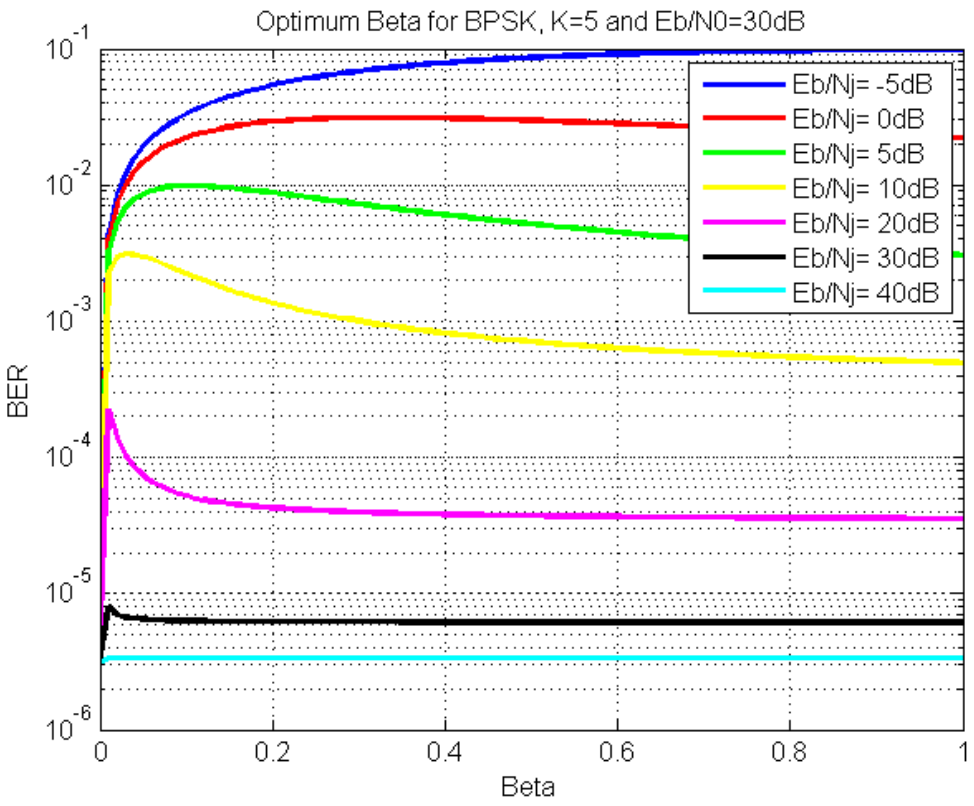

Fig. 24. BER versus PBTJ fraction β for BPSK under Rician fading of factor $K = 5$, $E_b/N_0 = 30\ dB$ with E_b/N_J as a parameter in dB.

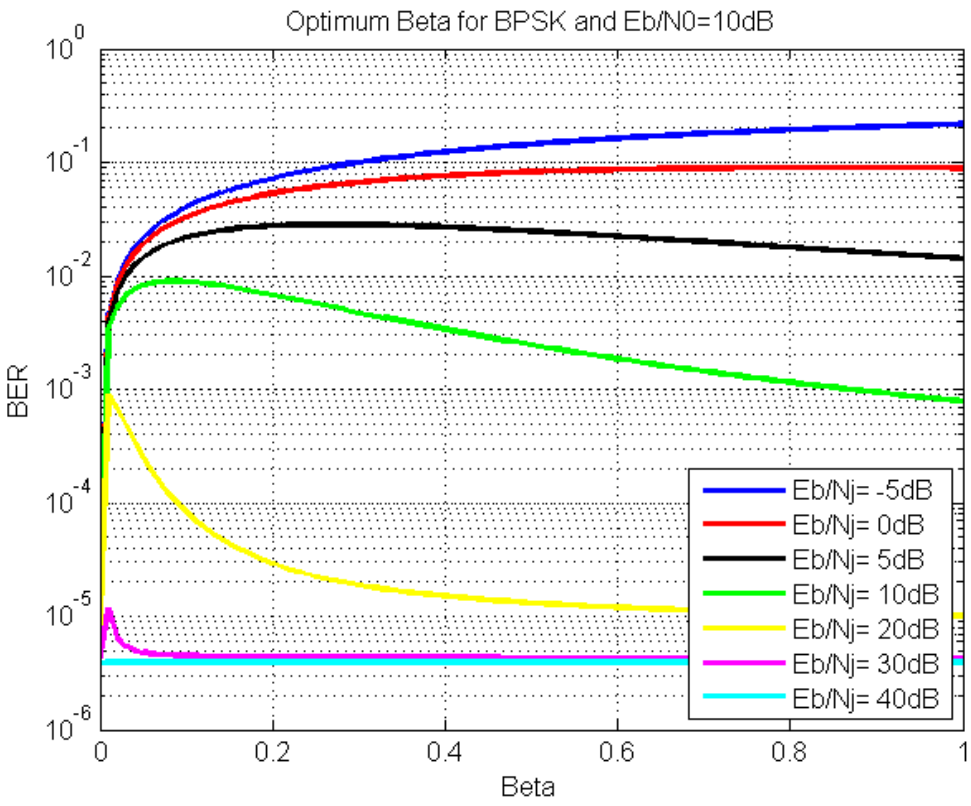

Fig. 25. BER versus PBTJ fraction β for BPSK under no fading and $E_b/N_0 = 10\ dB$ with E_b/N_J as a parameter in dB.

It can be seen in Figs. 3 to 15 that when NLOS is dominant, i.e., K is small such as 0.1 or 0.9, the BER worsens as the PBTJ fraction β increases. Thus, the optimum jamming fraction would be 1. In other words, wideband PBTJ is more effective against the desired user than narrowband PBTJ. However, as shown in Figs. 22 to 25, when no fading but only AWGN and PBTJ are present in the system (in other words only the LOS component is present with $K = \infty$) or when Rician fading of a strong LOS component with $K = 5$, the optimum PBTJ jamming fraction becomes smaller than 1 as E_b/N_J increases (i.e., as jamming power gets weaker). For example, the optimum beta is around 0.3 in Fig. 25 when $E_b/N_J = 5\ dB$, $E_b/N_0 = 10\ dB$, and BPSK is used and no fading. And the optimum beta decreases from 0.3 to 0.08 when E_b/N_J increases from $5\ dB$ to $10\ dB$. Hence, a narrower PBTJ would be more effective than a wider PBTJ when the jamming power gets weaker for the AWGN or for the AWGN plus Rician fading of a strong LOS

component such as $K = 5$ and PBTJ channel. The optimum beta shown in Figs. 22 to 25 agree with those obtained through numerical searches using (32).

VI. Conclusions

We derived an exact symbol error rate expression for the FHSS system under partial-band tone jamming and Rician fading environments. The expression can be easily extended to other fading environments such as Rayleigh and Nakagami and other modulations such as MQAM. In addition, we studied the optimal weighting coefficients, called beamforming coefficients, to minimize the SER when channel coefficients are available. Furthermore, we presented an implicit expression of the worst PBTJ fraction ratio, which maximizes the SER of the FHSS system, and verified that the analytically derived optimal PBTJ fraction ratio agrees with those obtained through numerical computations. It was found that when the NLOS component in Rician fading is stronger than the LOS component, in other words when Rician factor K is small such as 0.1 and 0.9, the worst PBTJ fraction ratio is 1. On the other hand, when Rician factor K gets larger than 1 and jamming power weakens, the optimum jamming fraction can be smaller than 1. For this case, narrowband PBTJ is more effective than wideband PBTJ. Results and observations in this paper would be useful in designing a future, efficient FHSS satellite and mobile communications system under PBTJ and fading or no-fading environments.

VII. Acknowledgment

This work was supported in part by the Air Force Summer Faculty Fellowship Program, the Air Force Research Laboratory (AFRL) under Grant FA9453-15-1-0308, and Asian Office of Aerospace R&D (AOARD) AFRL under Grant FA2386-14-1-0026. The views and conclusions contained herein are those of the authors and should not be interpreted as necessarily representing the official policies or endorsements, either expressed or implied, of the AFRL or the U.S. Government.

References

[1] Usuda, M., Ishikawa, Y., Onoe, S., "*Optimizing the number of dedicated pilot symbols for forward link in W-CDMA systems*," Vehicular Technology Conference Proceedings, 2000. VTC 2000-Spring Tokyo. 2000, pp. 2118–2122, vol.3, May 2000.

[2] Love, R., Ghosh, A., Xiao, W., and Ratasuk, R., "Performance of 3GPP high speed downlink packet access (HSDPA)," IEEE 60th Vehicular Technology Conference, VTC2004-Fall, pp. 3359–3363 Vol. 5, Sept. 2004.

[3] Abeta, S., "Toward LTE commercial launch and future plan for LTE enhancements (LTE-Advanced)," IEEE International Conference on Communication Systems (ICCS), pp. 146–150, Nov. 2010.

[4] Gong, K.S, "Performance of Diversity Combining Techniques for FH/MFSK in Worst Case Partial Band Noise and Multi-Tone Jamming," IEEE Military Communications Conference, MILCOM 1983 (Volume: 1), pp. 17–21, Oct. 1983.

[5] Viswanathan, R., and Taghizadeh, *K.*, "Diversity combining in FH/BFSK systems to combat partial band jamming," *IEEE Transactions on Communications*, Vol 36, Iss. 9, pp. 1062–1069, Sept. 1988.

[6] Popper, C., Strasser, M., and Capkun, S., "Anti-jamming broadcast communication using uncoordinated spread spectrum techniques," *IEEE Journal on Selected Areas in Communications*, Vol. 28, Iss. 5, pp. 703–715, June 2010.

[7] Gass, J.H., Jr., and Pursley, M.B., "A comparison of slow-frequency-hop and direct-sequence spread-spectrum communications over frequency-selective fading channels," *IEEE Transactions on Communications*, Vol. 47, Iss. 5, pp. 732–741, May 1999.

[8] Flikkema, P., "Spread-spectrum techniques for wireless communication," *IEEE Signal Processing Magazine*, Vol. 14, Iss. 3, pp. 26–36, May 1997.

[9] Fried, W.R., "Principles and Simulation of JTIDS Relative Navigation*," IEEE Transactions on Aerospace and Electronic Systems*, Vol. AES-14, Iss. 1, pp. 76–84, Jan. 1978.

[10] Sabatini, R., Aulanier, L., Rutz, H., Martinez, M., Foreman, L., Pour, B., and Snow, S., "Multifunctional information distribution system (MIDS) integration programs and future developments," IEEE Military Communications Conference, MILCOM 2009.pp. 1–7, Oct. 2009.

[11] Andrusenko, J., Miller, R.L., Abrahamson, J.A., Merheb Emanuelli, N.M., Pattay, R.S., and Shuford, R.M. , "VHF General Urban Path Loss Model for Short Range Ground-to-

Ground Communications," IEEE Transactions on Antennas and Propagation, Vol. 56, Iss. 10, pp. 3302–3310, Oct. 2008.

[12] Rodriguez Bejarano, J.M., Yun, A., and De La Cuesta, B., "Security in IP satellite networks: COMSEC and TRANSEC integration aspects," Advanced Satellite Multimedia Systems Conference (ASMS) and 12th Signal Processing for Space Communications Workshop (SPSC), pp. 281–288, Sept. 2012.

[13] Pursley, M.B., and Russell, H.B., "Adaptive forwarding in frequency-hop spread-spectrum packet radio networks with partial-band jamming," *IEEE Transactions on Communications*, Vol. 41, Iss. 4pp. 613–620, Apr. 1993.

[14] Chun-Meng, Su, and Milstein, L.B., "Analysis of a coherent frequency-hopped spread-spectrum receiver in the presence of jamming," *IEEE Transactions on Communications*, Vol. 38, Iss. 5, pp. 715–726, May 1990.

[15] Chau, Y.A., and Mason, L.J., "Error probability for FH/MDPSK in multitone jamming, fast Rician fading, and Gaussian noise," *IEEE Transactions on Communications*, vol. 43, no. 2/3/4, pp. 545–553, Feb./Mar./Apr. 1995.

[16] Chau, Y.A. "Optimal partial decision diversity for frequency-hopped satellite communications in shadowed Rician fading channel with partial-band jamming," *Proceedings of IEEE 1993 Region 10 Conference Computer, Communication, Control and Power Engineering, TENCON '93*, Beijing, China, Vol. 3, pp. 123–126, Oct. 19–21, 1993.

[17] Hassan, Amer A., Stark, Wayne E., and Hershey, John E., "Error Rate for optimal Follower Tone Jamming," *IEEE Transactions on Communications*, Vol. 44, No. 5, pp. 546–548, May 1996.

[18] Glaser, M., Greiner, K., Hilburn, B., Justus, J., Walsh, C., Dallas, W., Vanderpoorten, J., and Chuang, Jo-Chieh, "Protected MILSATCOM design for affordability risk reduction (DFARR)," IEEE Military Communications Conference, San Diego, CA, November 18–20, 2013.

[19] Cook, K. L. B., "Current wideband MILSATCOM infrastructure and the future of bandwidth availability," *IEEE Aerospace and Electronics Systems Magazine*, pp. 23–28, 2008.

[20] Simon, M.K., and Alouini, M.S., *Digital Communication over Fading Channels*, Wiley-IEEE Press, 2nd edition, December 6, 2004.

[21] Simon, M.K., and Alouini, M.S. "A unified approach to the performance analysis of digital communications over generalized fading channels," *IEEE Proceedings*, pp. 1860–1877, Sept. 1998.

[22] Goldsmith, A., *Wireless Communication*, 5th ed., Cambridge University Press, 2012.

[23] Craig, J., "New, simple, exact result for calculating probability of error for two-dimensional signal constellations," *Proceedings Military Communications Conference*, pp. 25.51–25.5.5, Nov. 1991.